JKAU: Earth Sci., **vol. 14,** pp. 57-90 (2002-2003 A.D. / 1423-1424 A.H.)

The Late Cretaceous Turabah Ring Dyke, Central Arabian Shield, Kingdom of Saudi Arabia – Geology, Geochemistry and Tectonic Significance

ISSAM YAHIA AL FILALI
Faculty of Earth Sciences, King Abdulaziz University, Jeddah, Saudi Arabia

Received: 2/10/2002 Revised: 5/5/2003 Accepted: 17/5/2003

ABSTRACT. The Turabah ring dyke, in the central Arabian Shield of Saudi Arabia, is a Late Cretaceous alkaline A-type granite. It was emplaced at shallow crustal levels in a Pan-African assemblage of calc-alkaline metavolcano-sedimentary association, syn-tectonic metagabbro-diorite, granodiorite-granite gneiss, tonalite gneiss and syenite. The metavolcanics and the metagabbro-diorite exhibit petrological and geochemical characteristics of mantle-derived island-arc rocks, which were formed by partial melting of a mantle wedge above subduction zone. The granodiorite-granite gneisses are calc-alkaline I-type granites. They and the metagabbro-diorite show continuous major and trace element trends, suggesting that the two suites are genetically related through fractional crystallization process. The tonalite gneisses possess low contents of REE (51-74 ppm), Zr (43-72 ppm), Rb (2-17 ppm), K_2O (0.35-1.14 wt. %), Nb (3-5 ppm) and have trace element patterns not modified greatly by fractionation. These chemical aspects may suggest their derivation via partial melting of lower crust.

The rocks of the Turabah ring dyke consist of subsolvus monzo-and syenogranites. They are geochemically evolved (SiO_2 = 68-77%), metaluminous to mildly peralkaline and display a within plate A-type geochemical signature with enrichment in Fe_2O_3 (1-4 wt %), Y (7-35 ppm), Nb (3-19 ppm), Rb (45-101 ppm), Zr (101-446 ppm) and depletion in CaO (0.5-1.9 wt %), MgO (0.02-0.6 wt %), Ba (14-820 ppm) and Sr (5-213 ppm). A model involving partial melting of a mafic lower continental crust in an extensional environment, to produce a granodioritic melt, can explain the origin of these rocks. Direct contamination of that granodioritic melt with an old continental crust followed by fractional crystallization played an important role in the evolution and chemical characterization of the Turabah A-type gran-

ites. The complex evolution history of the area may be reflected in the formation quasi-oval fractures, along which the fractionated melt was intruded, giving rise to the ring structure in the area.

Introduction

It is now widely accepted that the crust of the Arabian-Nubian Shield (ANS) of NE Africa and Arabia was generated during the Pan-African orogenic event (950-550 Ma, Kröner, 1985). The general tectonic model for the entire ANS involves progressive cratonization through formation of an oceanic crust, subduction, magmatic arc development and collision between arc complexes to assemble a continental shield (Frisch and Al Shanti, 1977; Kröner *et al.,* 1987; Stern, 1994). Four main rock assemblages, namely: 1) an arc assemblage, 2) an ophiolite assemblage, 3) a gneiss assemblage and 4) granite intrusions, characterize the crust of the ANS. The syn-tectonic granite intrusions are mainly calc-alkaline diorite-tonalite-trondhjemite-granodiorite-granite, which are mainly deformed and emplaced between 900 and 700 Ma (Jackson, 1986). Towards the end of the Pan-African event (at about 600 Ma), the ANS witnessed the abundant emplacement of post-orogenic and anorogenic alkaline magmatism, which intruded the subduction-related Pan-African basement rocks (Vail, 1985, Harris, 1985). Most of these alkaline rocks, with A-type characteristics occur in the form of well-developed ring structures, stocks, plugs and ring dykes, which vary in age between closing the island arc activity at the end of the Pan-African orogeny and opening of the Red Sea (Vail, 1985).

In the Arabian Shield, granitoid plutons emplaced at various crustal levels make up about 40% of the exposed upper Proterozoic basement rocks (Stoeser and Elliott, 1980). Over 50 alkaline discrete igneous complexes (Fig. 1), are characterized by predominance of silica saturated acidic rocks, shallow level of emplacement, common presence of ring structure and ring dykes, and a tendency to include alkaline and peralkaline variants (Stoesser and Elliott, 1980; Harris, 1985). The period of emplacement of most of these complexes is mainly restricted to the time period between 630 and 550 Ma (Harris, 1985). However, there are few ring structures that post-date this time period of which the investigated Turabah ring dyke (117 ± 0.4 Ma, Radain *et al*., 1988) represent the latest plutonic activity reported from the Arabian Shield.

The Wadi Turabah area is an exposure of Proterozoic basement in the north-central part of the southern Asir terrane where various volcanic and plutonic rocks are exposed (Fig. 2). It comprises metavolcano-sedimentary association, highly deformed felsic plutonic rocks and granite ring dyke. This study focuses on the Turabah igneous complex, especially the ring dyke granite that intrudes the Pan-African regionally metamorphosed rocks. New field and geochemical

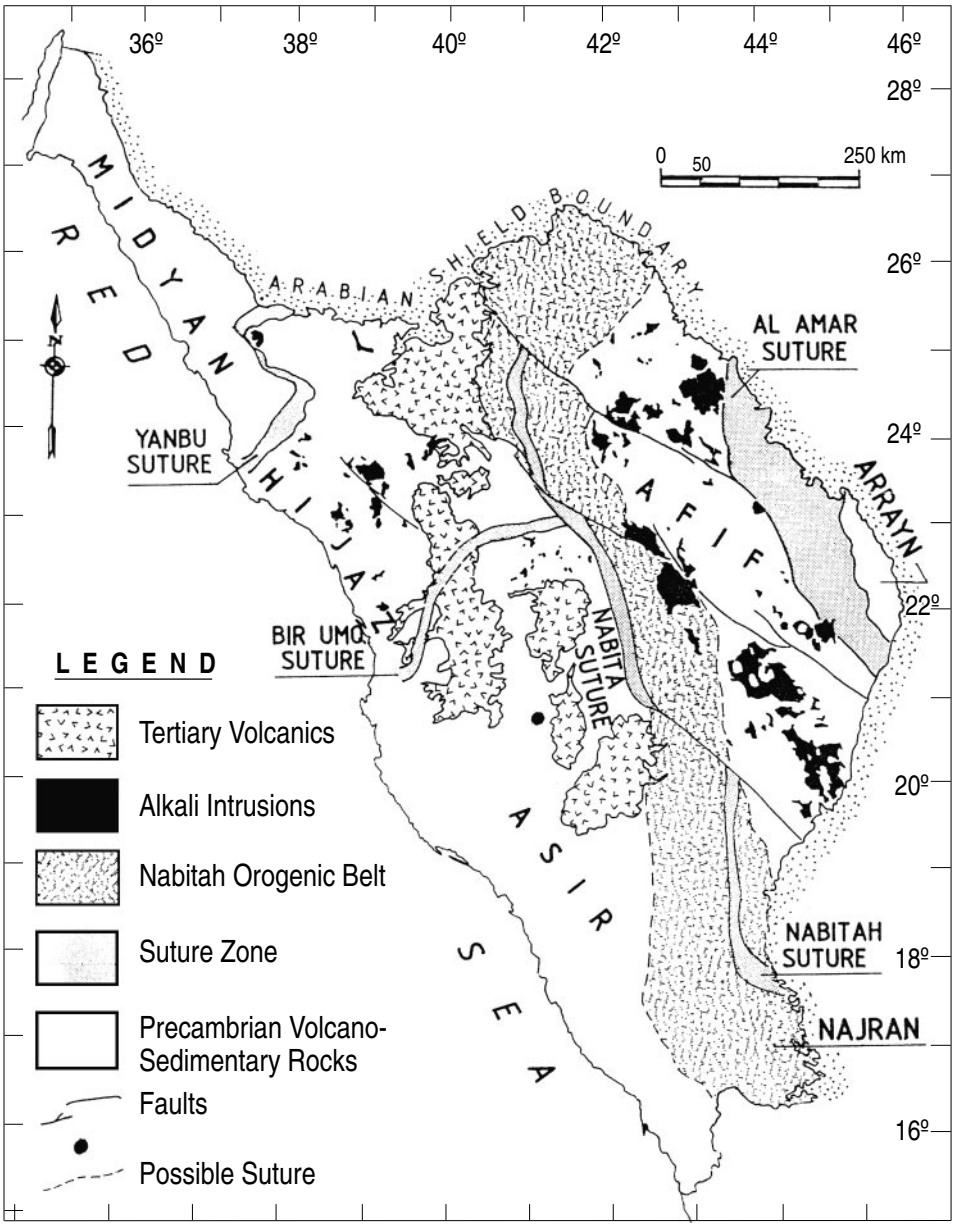

FIG. 1. Map showing the distribution of alkali intrusions in the Arabian Nubian Shield and the location of the study area.

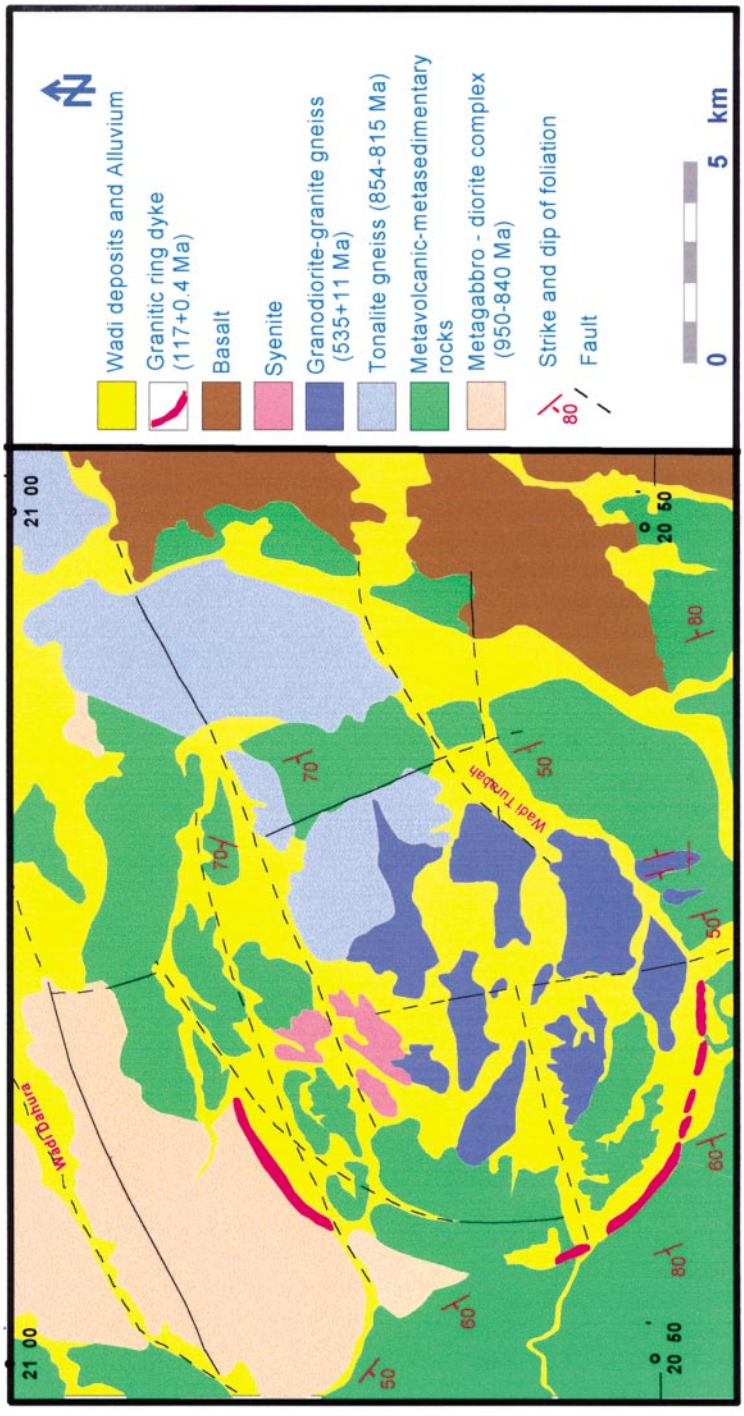

FIG. 2. Geologic map of Wadi Turabah area based on the regional geologic map of Cater and Johnson (1987).

data are presented and used to shed light on its magmatic and tectonic evolution. Further, the magma source from which the rocks of the ring dyke granite was derived is discussed

2. Geological Setting

2.1. General Setting and Previous Work

Models for the evolution of the Arabian Shield (Stoeser and Camp, 1985) indicate its development through a series of orogenesis associated with collisional events along suture zones between five microplates. Two microplates in the eastern Shield (the Afif and Ar Rayn terranes) are of continental affinity and have been dated at 2000 – 1600 Ma (Stacey and Stoeser, 1983). The other three microplates (Asir in the south, Hijaz in the center and Midyan in the north) are ensimatic island arc terranes of 940 – 700 Ma age (Stoeser and Camp, 1985). The study area lies within the Asir ensimatic microplate and in the northern part of Jabal Ibrahim quadrangle (sheet 20E, Cater and Johnson, 1987). According to Cater and Johnson (1987), four principal rock units crop out in the Jabal Ibrahim quadrangle. From the oldest to youngest, these are: 1) primitive intraoceanic island arc assemblage of tholeiitic basalt, Na-rich dacite-rhyolite (Baish and Bahah groups) and diorite-tonalite intrusions, which developed between 950 – 840 Ma (Aldrich, 1978; Marzuki *et al.*, 1982; Kroner *et al.,* 1984); 2) more evolved island arc assemblage of tholeiitic basalt, calc-alkaline andesite to rhyolite (Qirshah and Khutnah formations) and diorite-tonalite intrusions, which have been dated at about 750 – 720 Ma (Fleck *et al.,* 1976, 1980; Bokhari and Kramers, 1981); 3) epiclastic rocks (Ablah Formation) which have been deposited unconformably upon the older arc assemblage (Cater and Johnson, 1987) after a period of deformation and regional metamorphism; 4) late- to post-orogenic granitoids which vary in age between 690 and 550 Ma (Radain and Nasseef, 1982; Radain *et al.,* 1987)

Geological mapping of the Wadi Turabah area was carried out by Greene and Gonzalez (1980) and reveals the presence of circular intrusive structure consisting of syenite-trondhjemite complex and other rock units. Divi *et al.* (1984) demonstrated that the Wadi Turabah area is occupied by highly deformed and polymetamorphosed Proterozoic association consisting of metavolcano-sedimentary association, tonalite-diorite, granite granodiorite, gabbro-diorite and syenite-trondhjemite. These units were intruded by a granite ring dyke, which is discordant to the deformation structures in the surrounding rock units, indicating its relatively younger age. Geochronological studies on felsic plutonic rocks of the Wadi Turabah area reveal that the deformed tonalite-diorite yield Rb/Sr ages between 854 ± 10 and 815 ± 13 Ma, whereas a post-orogenic biotite granite pluton yield Rb/Sr age of 552 ± 20 Ma (Radain and Nasseef, 1982; Ra-

dain *et al.,* 1987). On the other hand, the highly deformed granodiorite-granite gneiss yields a Rb/Sr errochron with an age of 535 ± 11 Ma with an initial ratio of 0.7037, and the ring dyke granite yields a Rb/Sr isochron age of 117 ± 0.4 Ma (MSWD = 0.01) and initial ratio of 0.7089 ± 0.0001 (Radain *et al.,* 1988).

2.2. Field Observation and Petrography

Based on the present field study and previous lithostratigraphy, the rocks in the Wadi Turabah area can be separated into six lithological units arranged chronologically as follows: metavolcano-sedimentary association, metagabbro-diorite, tonalite gneiss, granodiorite-granite gneiss, syenite and ring dyke granite. The area has experienced multiple deformation and metamorphism caused by complex tectonic events during the Pan-African orogeny. The volcano-sedimentary association and the metagabbro-diorite are deformed and metamorphosed in the greenschist and amphibolite facies. The granodiorite-granite gneiss, the tonalite gneiss and the syenite are highly deformed as indicated by mineral foliations especially the mafic ones. Except for local development of low-temperature mineral deformation (undulose extinction in quartz and deformed lamellae in plagioclase) the ring dyke granite is the only undeformed granite variety in the area.

2.2.1. Metavolcano-sedimentary association

The metavolcanics represent the oldest unit, which occupies a large exposure to the west and southwest of the map area (Fig. 2.). It consists of a highly deformed succession of mafic to intermediate volcanic rocks that have been regionally metamorphosed in the amphibolite to the greenschist facies. This rock unit is similar to volcanic rocks of the Baish and Bahah groups that have been considered as immature oceanic island arc (Ramsay *et al.,* 1981). It consists of hornblende schist, actinolite-chlorite schist, and mica schist. The hornblende schists are mainly fine-grained (in the southern part) to medium-grained (in the northern part) and consist of hornblende and partly sericitized plagioclase feldspar (An_{15-30}), with minor quartz and accessory opaques. Hornblende is quite fresh and occasionally contains poikiloblastic inclusions of rounded plagioclase. The plagioclase and hornblende crystals show a general tendency to lay parrallel to each other, imparting to the rock its foliated nature. Chlorite schists consist of sericitized plagioclase, chlorite, epidote and actinolite, whereas mica schists are made up of plagioclase, biotite, muscovite and quartz. Based on the evidence of some preserved primary structures, the hornblende schist is considered to be meta-basalts and meta-andesites and the actinolite-chlorite schist and mica schist, are presumed to be derived from felsic lavas and tuffs (Cater and Johnson, 1987).

The metasediments are represented by pelitic schists (metagreywackes) that consist of poorly sorted and subrounded quartz and feldspar grains set in a recrystallized matrix of quartz, feldspars, biotite, actinolite and chlorite. Quartzite, phyllite, slate and marble, in relatively decreasing order of abundance, are also encountered within the metasedimentary association. Although primary depositional features are mostly obliterated, bedding and lamination are locally observed.

2.2.2. Granodiorite-granite gneiss

The granodiorite-granite gneiss crops out in the central part of the study area, forming the core of the ring complex (Fig. 2). The rocks of this granitoid suite intruded the volcano-sedimentary association. They are homogeneous, coarse- to medium-grained, and gray to whitish grey and are highly deformed and sheared. A foliation defined by the alignment of biotite and hornblende clots gives the rock a gneissose appearance in some parts. This foliation is conformable with that of the volcano-sedimentary association. The granodiorite-granite gneiss shows variation in the proportions of the alkali feldspar, quartz and mafic minerals. Felsic minerals include oligoclase (40-50%), quartz (15-20%), microcline and orthoclase (13-20%). Dark brown biotite (3-7%) and green hornblende (5-10%) form the mafic clots that define the rock foliation. The granodiorite gneiss locally grade to granitic gneiss with similar mineralogical composition but with higher abundance in quartz (≈ 30%) and alkali feldspar (25%). Apatite, sphene and zircon in addition to opaque minerals are the common accessory minerals in the granodiorite gneiss, except sphene that is rare in the granitic gneiss.

2.2.3. Metagabbro-diorite

The metagabbro-diorite body occurs in the northern part of the area. It intrudes the volcano-sedimentary association and the granodiorite-granite gneiss. Typical gabbroic rocks contain 45-55% euhedral to subhedral zoned plagioclase crystals variably altered to sericite and epidote. Plagioclase ranges from labradorite to dominant andesine. Hornblende is the main mafic mineral in the gabbroic rocks with modal content of about 25-40%. It occurs as medium-grained subhedral twinned crystals as well as poikilitic patchy grains with inclusions of plagioclase, magnetite and apatite. Augite (about 6%) is present in some varieties as small subhedral to anhedral grains and also as remnants in hornblende. Diorite is composed predominantly of andesine and hornblende, with minor amounts of quartz, biotite, and K-feldspar.

2.2.4. Tonalite gneiss

The tonalite gneiss occurs as patches and isolated hills in the central part of the study area, which occupied mainly by sandy plains. Tonalite gneisses are

coarse- to medium-grained, foliated and have conformable boundaries with the surrounding rocks They show more or less mineralogical similarity to the granodiorite-granite gneisses except that they are enriched in plagioclase and biotite with no or little hornblende. Their felsic minerals include andesine (55%), quartz (22%), and microcline microperthites (18%). Dark brown subhedral biotite flakes (5%) are the main mafic minerals. Accessory minerals include magnetite, sphene, apatite and zircon.

2.2.5. Syenite

The syenite also occurs as small masses in the central part of the ring complex, locally grade to quartz syenite. The rocks are coarse-grained, massive and whitish gray with equigranular hypidiomorphic texture. It consists of abundant orthoclase and microcline (70-80%), quartz (5-20%) and plagioclase (3-5%) together with minor amount of hornblende and accessory sphene, zircon, apatite and allanite.

2.2.6. Ring dyke granite

The wadi Turabah ring dyke represents the youngest intrusion in the study area. It crops out as discontinuous semi-circualr ring structure of approximately 13 km diameter. It intrudes the metavolcano-sedimentary rocks with sharp intrusive and discordant contact. It is predominantly pale pink to red, massive and equigranular, but porphyritic outcrops are also observed. It is subsolvus granite consisting of quartz (40%), orthoclase and microcline (43%), plagioclase (An_{10-15}) (12%), together with biotite and hornblende (5%). Accessory minerals are magnetite, allanite, sphene, apatite and zircon. Poikilitic plagioclase inclusions in some large quartz crystals are common. Late stage muscovite and chlorite replacing earlier biotite and hornblende are occasionally observed.

3. Geochemistry

3.1. Sample Set and Analytical Techniques

Based on the petrographic investigations, 29 representative samples covering the different rock varieties were selected for major and trace element analyses. Major element compositions and Sc, Ba, and Ni abundances were determined by inductively coupled plasma-atomic emission spectrometry (ICP-AES). The remainder of trace elements and the rare earth elements (REE) were determined by inductively coupled plasma-mass spectrometry (ICP-MS). All the analyses have been carried out at the ACME Analytical Laboratories Ltd., Canada. Analytical precision, as calculated from replicate analyses, is 0.5% for major elements and varies in the range of 3-5% for trace elements of >100 ppm, 2-10% for trace elements of 10-100 ppm, and 5-20% for trace elements of <10 ppm. The analytical data is given in Table 1.

TABLE 1. Chemical data of the Wadi Turabah volcano-plutonic complex.

Sample rock	T-6	T-8	T-9	T-12	T-14	T-16	T-23	T-24	T-25	T-28	T-29
	Metavolcanic rocks			Granodiorite-granite geneisses			Metagabbro-diorite				
SiO_2	59.03	56.36	67.16	70.58	72.90	72.42	56.74	49.44	59.15	58.12	54.39
TiO_2	0.17	1.50	0.46	0.53	0.43	0.40	1.77	0.85	1.71	0.72	0.75
Al_2O_3	9.75	13.29	14.52	13.48	12.69	13.38	13.41	16.27	13.28	18.61	19.61
Fe_2O_3	11.63	9.86	4.98	3.44	3.07	2.99	9.83	8.04	9.45	5.88	6.46
MnO	0.21	0.15	0.12	0.08	0.06	0.07	0.15	0.13	0.15	0.09	0.12
MgO	8.92	6.61	1.87	0.58	0.44	0.45	6.64	8.10	5.97	2.85	3.25
CaO	8.21	5.63	3.59	2.03	1.25	1.51	5.76	12.63	5.41	6.61	7.35
Na_2O	0.92	3.04	3.55	4.05	3.67	3.78	2.69	2.57	2.51	5.86	5.77
K_2O	0.25	1.52	2.77	3.54	3.65	3.83	0.97	0.40	0.50	0.41	0.38
P_2O_5	0.03	0.50	0.13	0.11	0.08	0.07	0.59	0.03	0.55	0.24	0.29
LOI	0.70	1.20	0.70	0.50	0.40	0.40	1.20	1.10	1.10	0.60	1.50
Sum	99.82	99.66	99.85	98.92	98.64	99.30	99.75	99.56	99.78	99.99	99.87
Co	46	43	8	4	4	3	42	51	39	17	21
Sc	52	20	18	14	8	7	19	29	19	12	14
V	236	171	27	21	18	16	152	172	154	112	115
Sn	1	1	2	2	1	1	2	2	2	3	3
W	11	30	31	9	23	1	9	17	39	13	20
Rb	2	32	59	50	49	50	21	16	10	2	3
Cs	0.1	1.0	0.9	0.5	0.5	0.7	0.7	2.3	0.5	0.5	1.3
Ba	77	615	710	655	462	616	624	95	348	234	238
Sr	90	688	440	208	142	177	772	675	710	1055	1126
Tl	0.1	0.4	0.2	0.3	0.3	0.3	0.2	0.5	0.5	0.5	0.4
Ga	9	17	13	19	18	19	16	17	17	21	23
Ta	0.1	0.8	0.5	0.8	0.4	0.3	0.5	0.2	1.1	0.1	0.3
Nb	1	8	4	14	9	8	8	2	10	2	3
Hf	0.5	4.0	2.3	11.1	8.5	8.8	2.4	1.3	4.6	1.6	0.8
Zr	10	159	75	461	330	363	94	43	175	69	33
Y	4	16	23	23	14	14	16	8	20	7	10
Th	0.2	3.2	1.4	6.4	6.5	4.7	3.8	0.1	5.9	0.1	0.1
U	0.1	1.4	0.6	2.2	1.7	1.6	1.6	0.1	3.9	0.1	0.1
La	1.5	24.0	10.9	66.8	70.2	78.7	17.7	3.3	24.2	4.8	7.0
Ce	2.7	53.5	24.3	144.1	147.2	159.6	44.4	7.8	57.0	11.0	17.3
Pr	0.36	6.85	3.25	17.43	16.56	17.62	6.50	1.21	7.79	1.67	2.51
Nd	1.7	27.6	14.8	63.1	59.3	60.0	28.3	6.3	34.4	8.2	12.1
Sm	0.50	5.30	3.10	10.10	7.90	7.60	5.60	1.80	6.50	2.00	2.60
Eu	0.15	1.52	1.14	1.03	0.63	0.85	1.77	0.78	1.61	0.96	1.22
Gd	0.40	4.32	3.62	6.78	5.23	4.17	4.60	1.86	5.24	2.08	2.90
Tb	0.09	0.58	0.55	0.90	0.61	0.54	0.60	0.26	0.71	0.25	0.36
Dy	0.66	3.48	4.24	5.31	3.74	3.22	3.52	1.70	3.97	1.61	2.10
Ho	0.16	0.61	0.84	0.95	0.59	0.53	0.62	0.33	0.78	0.26	0.41
Er	0.39	1.71	2.72	2.48	1.57	1.56	1.65	0.94	2.03	0.75	1.03
Tm	0.07	0.23	0.34	0.33	0.20	0.21	0.22	0.12	0.29	0.08	0.14
Yb	0.45	1.26	2.39	2.44	1.33	1.49	1.60	0.86	2.01	0.60	0.87

Lu	0.07	0.20	0.41	0.35	0.20	0.19	0.22	0.31	0.31	0.08	0.12
REE(t)	9.2	131.0	73.0	322.0	315.0	336.0	117.0	27.0	147.0	34.0	51.0
(La/Yb)n	2.30	12.90	3.10	18.50	35.60	35.70	7.50	2.60	8.10	5.40	5.40
(Eu/Eu*)	1.02	0.97	1.04	0.40	0.30	0.46	1.10	1.30	0.84	1.40	1.35

Fe_2O_3 is the total Fe as Fe_2O_3.

TABLE 1. Contd.

Sample rock	T-13	T-15	T-19	T-20	T-21	T-22	T-1	T-2	T-3	T-4	T-5
	Tonalite gneisses			Syenite			Ring dyke granite				
SiO_2	72.41	71.63	72.72	61.95	61.28	62.04	75.93	76.99	76.66	74.68	74.50
TiO_2	0.37	0.29	0.34	0.73	0.80	0.83	0.12	0.07	0.09	0.14	0.12
Al_2O_3	13.17	12.59	12.36	17.89	17.70	18.27	11.88	11.54	11.97	11.73	12.60
Fe_2O_3	4.17	5.35	3.74	2.09	2.97	2.32	0.99	1.39	1.70	3.35	1.71
MnO	0.11	0.13	0.05	0.04	0.07	0.04	0.03	0.04	0.03	0.06	0.04
MgO	0.78	1.03	1.52	0.48	0.69	0.51	0.08	0.07	0.02	0.04	0.14
CaO	3.59	4.29	5.21	1.47	1.35	1.16	0.58	0.49	0.47	0.65	1.24
Na_2O	3.65	3.38	3.14	6.95	6.42	7.07	3.40	3.59	3.85	5.10	3.58
K_2O	1.14	0.46	0.35	5.51	5.82	5.50	6.02	5.54	4.88	3.88	4.87
P_2O_5	0.11	0.10	0.09	0.03	0.11	0.05	0.01	0.01	0.01	0.01	0.01
LOI	0.40	0.60	0.50	1.50	1.10	0.80	0.90	0.20	0.30	0.30	1.10
Sum	99.90	99.85	100.0	98.64	98.31	98.59	99.94	99.93	99.98	99.94	99.91
Co	5	11	7	3	3	3	4	4	1	3	4
Sc	15	21	26	5	6	6	2	5	3	5	3
V	21	48	76	16	23	24	3	3	3	3	3
Sn	2	1	2	2	2	2	2	1	6	6	6
W	1	68	42	6	10	3	110	95	2	75	82
Rb	17	7	2	26	36	24	80	92	101	80	69
Cs	0.6	0.1	0.1	0.4	0.2	0.2	0.9	0.6	0.6	0.9	0.6
Ba	337	755	296	2052	2508	904	52	16	32	32	226
Sr	379	287	260	281	267	74	22	6	6	8	62
T1	0.2	0.2	0.2	0.2	0.3	0.2	0.3	0.3	0.4	0.3	0.2
Ga	12	12	11	19	20	21	20	22	23	28	21
Ta	0.4	0.6	0.6	0.4	0.3	0.4	1.6	1.1	0.9	1.7	1.6
Nb	3	3	5	8	6	9	8	7	11	19	8
Hf	1.6	1.5	2.4	13.3	12.4	14.8	3.9	4.7	6.4	7.4	5.6
Zr	56	43	72	841	812	950	115	159	189	216	185
Y	22	24	28	11	12	13	13	18	20	35	17
Th	1.1	0.4	0.9	0.3	0.4	2.4	5.8	3.8	7.3	11.4	8.7
U	0.6	0.3	0.5	0.2	0.3	0.2	1.6	1.6	3.1	4.2	3.5
La	11.1	6.3	5.8	28.3	28.5	177.1	45.9	22.9	25.0	36.3	38.8
Ce	25.0	14.8	16.5	55.8	54.7	368.2	104.3	67.8	72.0	102.0	87.3
Pr	3.37	2.11	2.54	7.61	7.30	43.54	12.01	8.29	8.97	14.19	10.13
Nd	15.2	9.9	12.1	33.0	31.7	150.9	45.8	35.3	36.0	60.50	39.20
Sm	3.50	2.50	2.90	6.30	5.50	19.30	6.20	8.40	7.30	14.20	6.60

Eu	1.17	0.69	0.84	3.50	3.30	4.08	0.22	0.05	0.05	0.05	0.29
Gd	3.66	3.20	4.08	4.81	4.48	9.74	3.11	5.74	4.52	9.67	4.21
Tb	0.55	0.49	0.66	0.58	0.48	0.78	0.42	0.85	0.71	1.36	0.57
Dy	4.00	4.12	4.95	3.17	3.17	4.54	2.74	4.83	4.11	7.41	3.30
Ho	0.78	0.90	1.03	0.49	0.51	0.58	0.50	0.78	0.84	1.40	0.65
Er	2.36	2.65	3.05	1.16	1.20	1.62	1.58	1.99	2.40	4.07	2.18
Tm	0.33	0.43	0.50	0.15	0.18	0.20	0.18	0.25	0.36	0.50	0.32
Yb	2.42	2.96	3.33	0.98	1.10	1.60	1.35	1.64	2.15	3.37	2.12
Lu	0.41	0.48	0.49	0.16	0.18	0.21	0.24	0.25	0.38	0.57	0.35
REE(t)	74.0	51.5	59.0	146.0	142.0	782.0	225.0	159.0	165.0	256.0	169.0
(La/Yb)n	3.10	1.40	1.20	19.50	17.50	74.00	23.00	9.40	7.80	7.30	12.40
(Eu/Eu*)	1.00	0.70	0.70	1.90	2.03	0.91	0.15	0.02	0.03	0.01	0.17

Fe_2O_3 is the total Fe as Fe_2O_3.

Table 1. Contd.

Sample rock	T-7	T-10	T-11	T-17	T-18	T-26	T-27
	Ring dyke granite						
SiO_2	74.95	72.88	68.15	76.72	71.08	76.78	76.40
TiO_2	0.09	0.46	0.51	0.22	0.41	0.08	0.09
Al_2O_3	12.73	12.04	15.36	11.20	13.53	12.19	11.73
Fe_2O_3	1.56	3.87	3.61	202	2.13	1.01	1.57
MnO	0.05	0.07	0.06	0.03	0.11	0.03	0.02
MgO	0.02	0.49	0.62	0.08	0.28	0.05	0.06
CaO	0.50	1.23	1.89	0.53	0.47	0.62	0.37
Na_2O	4.12	3.22	4.30	2.66	5.43	3.86	3.02
K_2O	4.49	3.53	3.99	5.06	4.77	4.46	5.25
P_2O_5	0.01	0.06	0.11	0.01	0.01	0.01	0.01
LOI	0.50	0.80	0.60	0.30	0.60	0.30	0.50
Sum	99.02	98.65	99.20	98.83	98.82	99.39	99.02
Co	1	4	5	6	2	2	3
Sc	5	7	9	3	3	3	1
V	3	19	22	3	11	3	3
Sn	2	1	2	1	2	2	3
W	1	1	7	103	1	115	90
Rb	70	52	59	45	79	49	74
Cs	0.7	0.7	0.7	0.1	0.3	0.4	0.6
Ba	14	440	820	102	969	46	49
Sr	5	130	213	12	54	12	21
Tl	0.4	0.3	0.3	0.2	0.2	0.6	0.6
Ga	20	18	22	17	19	18	18
Ta	0.7	0.7	0.6	1.1	0.7	1.2	1.2
Nb	6	11	10	5	11	3	4
Hf	2.9	10.8	10.1	7.1	9.2	5.9	4.3
Zr	101	423	446	274	436	199	135

Y	12	25	16	7	15	9	7
Th	5.6	7.8	2.2	10.4	2.3	2.9	5.5
U	1.5	3.0	1.1	1.3	0.8	1.7	1.8
La	41.7	95.5	32.8	96.4	59.0	24.1	6.6
Ce	107.5	195.4	72.9	187.9	85.9	56.2	27.4
Pr	14.36	22.60	9.31	20.53	13.99	6.90	1.64
Nd	52.5	80.4	35.5	71.9	50.5	25.2	5.6
Sm	9.00	11.60	6.40	8.60	7.30	3.80	1.00
Eu	0.05	0.66	0.85	0.20	1.61	0.11	0.07
Gd	4.86	7.33	5.40	4.39	5.15	2.43	0.96
Tb	0.58	0.87	0.66	0.50	0.59	0.34	0.18
Dy	3.29	5.27	3.69	2.50	3.16	1.95	1.20
Ho	0.50	0.94	0.63	0.32	0.58	0.35	0.26
Er	1.38	2.59	1.82	0.78	1.52	0.99	0.90
Tm	0.18	0.35	0.22	0.08	0.20	0.15	0.13
Yb	1.23	2.42	1.62	0.61	1.42	1.25	0.87
Lu	0.21	0.38	0.25	0.10	0.23	0.19	0.16
REE(t)	237.0	426.0	172.0	395.0	231.0	124.0	47.0
(La/Yb)n	23.0	27.0	14.0	106.0	28.0	13.0	5.1
(Eu/Eu*)	0.02	0.02	0.44	0.10	0.80	0.11	0.22

Fe_2O_3 is the total Fe as Fe_2O_3.

3.2. Results

For simplicity, the Turabah igneous complex will be divided into two groups according to field relations and metamorphic grade. These two groups are (1) the metavolcanics, syn-tectonic igneous complex (granite gneiss, metagabbro-diorite, tonalite-granodiorite gneiss) and syenite, and (2) post-tectonic ring dyke granite.

3.2.1. Geochemistry of the metavolcanics and syn-tectonic igneous complex

On the SiO_2 vs Na_2O+K_2O classification diagram (Fig. 3a) of Le Bas *et al.,* (1986), the chemical composition of the metavolcanics indicates that they range from basaltic andesite to andesite and dacite compositions. The metagabbro-diorite rocks have a composition similar to basalt, basaltic andesite and andesite whereas the granite gneiss and the tonalite gneiss plot in the rhyolite and dacite fields, respectively. The syenites lie within the trachyte field. Based on the Ab-An-Or ternary diagram of O'Connor (1965) (Fig. 3b), the studied granitoids are clearly separated into three suites. The tonalite gneiss is characterized by relatively high An contents and is classified as tonalite. The granite gneiss and the syenite have a relatively lower An content and are generally classified as granites. All the rock varieties are sub-alkaline, except the syenite which is alkaline, as shown in the SiO_2 vs Na_2O+K_2O diagram (Fig. 4a) of Irvine and Baragar (1971). The metavolcanics and the metagabbro-diorite have transitional tholeiit-

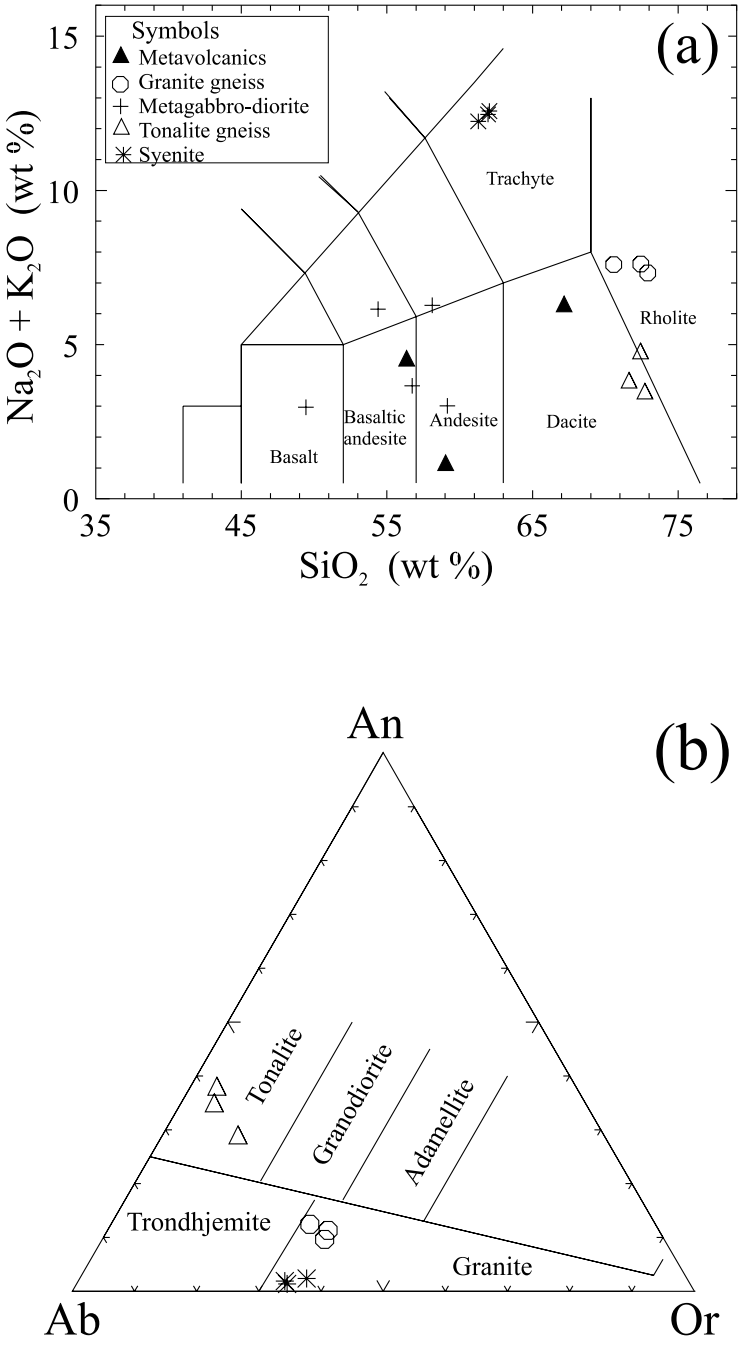

FIG. 3. Chemical classification of the examined syn-tectonic igneous assemblage according to: (a) SiO_2 versus $Na_2O + K_2O$ (TAS) diagram of Le Bas *et al.* (1986); (b) Ab-An-Or ternary diagram with the different fields from Barker (1979).

ic to calc-alkaline magma type (Fig. 4b) whereas the granite gneiss and the tonalite gneiss are calc-alkaline.

The metavolcanic rocks show chemical composition (Table 1) characterized by wide range of SiO_2 (56.4-67.2%), Al_2O_3 (9.8-14.5%), $Fe_2O_3^t$ (11.6 – 5%),

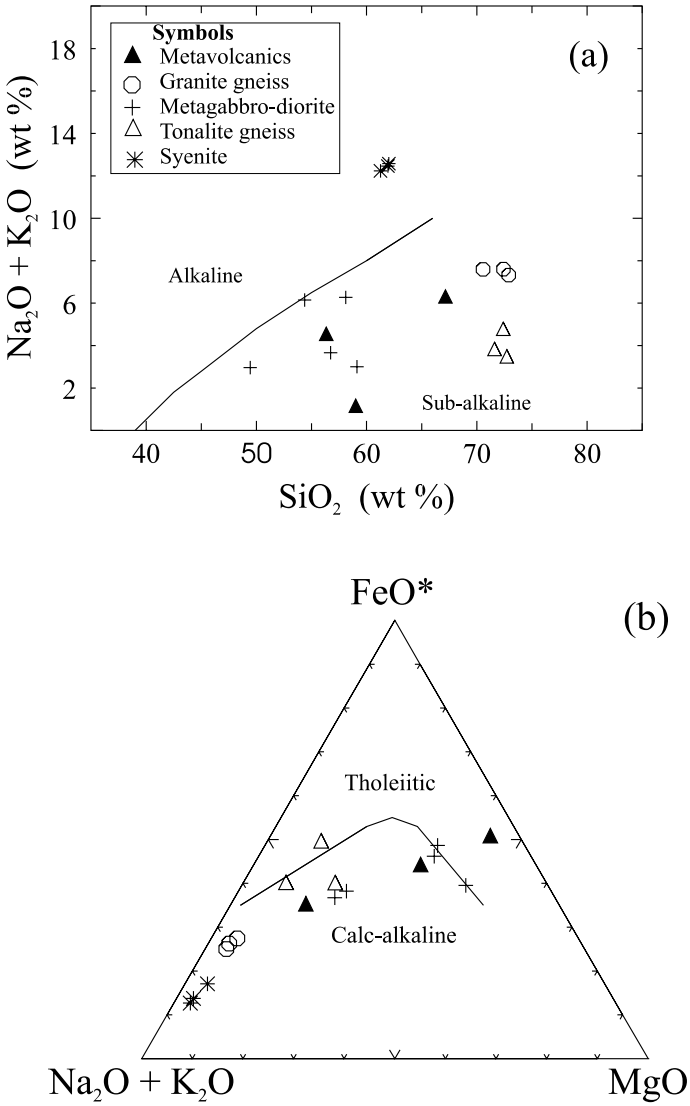

FIG. 4. (a) SiO_2 vs $Na_2O + K_2O$ variation diagram; the alkaline and subalkaline fields are after Irvine and Baragar (1971), (b) AFM ternary diagram with the tholeiitic and calc-alkaline fields from Irvine and Baragar (1971). Symbols as in Fig. 3.

MgO (8.92 – 1.87%), CaO (8.21 – 3.6%), TiO_2 (1.5 – 0.17%), Sc (52 – 18 ppm), Rb (2-59 ppm), Ba (77-710 ppm) and Sr (90-688). The analyzed samples have low total REE contents (9-131 ppm), poorly-fractionated REE patterns (Fig. 5a) with (Ce/Yb)n ratio between 2.3 – and 12 with no significant Eu anomalies (Eu/Eu* = 1.04 – 0.97). MORB normalized patterns of these rocks are of negative slope with LILE-enriched and Nb depletion (Fig. 6a).

The metagabbro-diorite samples (SiO_2 = 49.4 – 8.1 wt %) show also wide variations in chemical composition (Table 1) particularly with respect to Al_2O_3

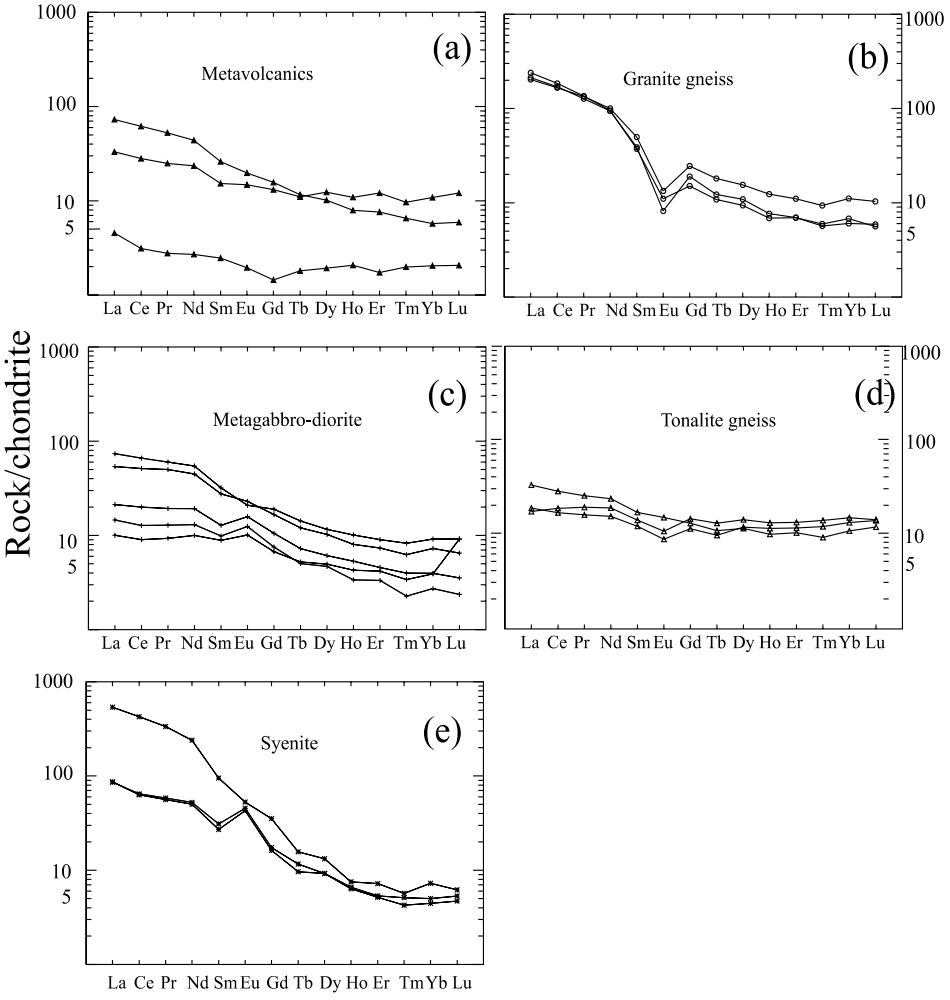

FIG. 5. Chondrite-normalized REE patterns (Sun, 1982) for the studied syn-tectonic igneous assemblage.

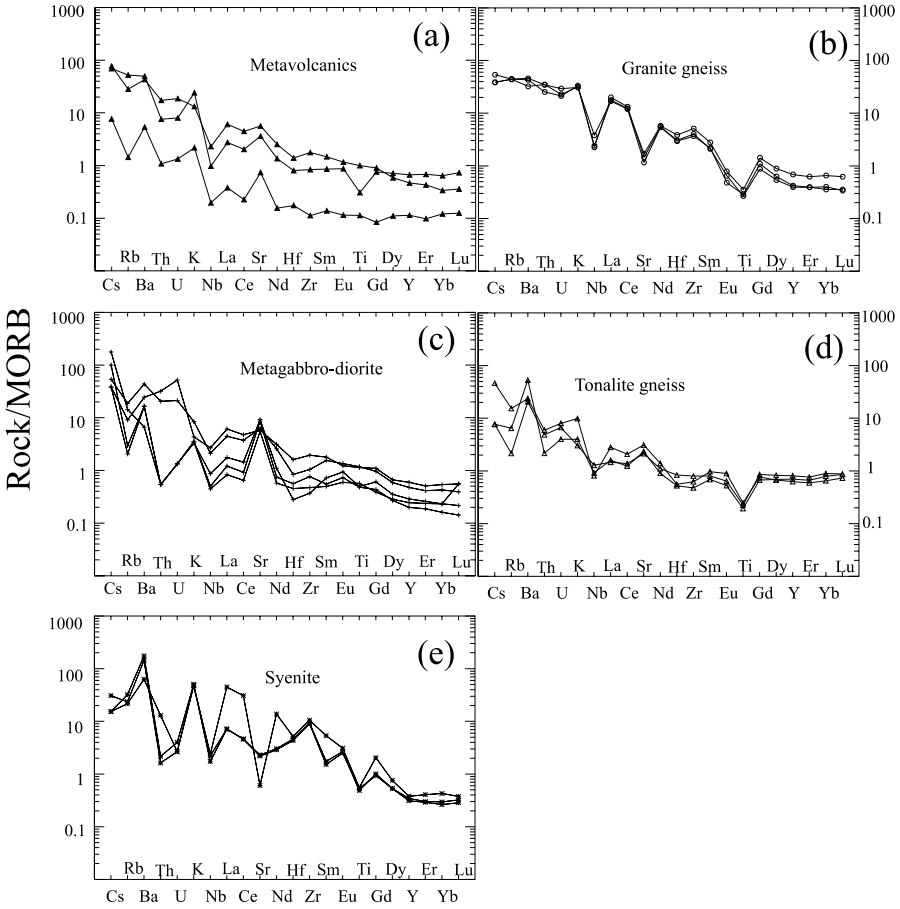

FIG. 6. N-MORB-normalized trace element plots (Sun and McDonough, 1989) for the studied syn-tectonic igneous assemblage.

(13.4-19.6%), CaO (5.4-12.6%), MgO (2.9-8.1), Rb (2-21 ppm), Ba (95-624 ppm), Sr (675-1126 ppm), Nb (2-10 ppm) and total REE (51-147 ppm). Plagioclase cumulates may account for the high Al_2O_3 (>18%) and CaO contents in some samples. Chondrite-normalized REE patterns of the metagabbro-diorite samples are LREE-enriched relative to HREE (Fig. 5c). The least evolved samples are characterized by relatively less fractionated patterns and positive Eu anomalies (Fig. 5c) whereas the highly evolved samples are characterized by more fractionated patterns and no significant Eu anomalies. MORB-normalized abundances of some selected elements are shown in Fig. 6c. The most striking feature of the metagabbro-diorite rocks is that all analyses are enriched in LILE and depleted in Nb, a feature often taken as indicative of subduction-related processes (Pearce, 1983). The positive Sr anomaly in some samples may be attributed to plagioclase cumulates.

The granite gneiss and the tonalite gneiss have a restricted variation in major and trace elements (Table 1). The chemical composition of the two rock types is indistinguishable for the major components SiO_2, TiO_2, Al_2O_3, Fe_2O_3, MgO, Na_2O and CaO. In contrast, the K_2O and the trace elements Sr, Rb, Ba, Nb, Zr and total REE (Table 1) show distinctly different contents for the two rock types. The tonalite gneiss is characterized by lower contents of these trace elements relative to the granite gneiss. REE patterns of the granite gneiss (Fig. 5b) are LREE-enriched and are highly fractionated (La/Yb) n = 36-19) with pronounced negative Eu-anomaly (Eu/Eu* = 0.3-0.5). MORB-normalized spidergrams of the granite gneiss (Fig. 6b) show well-defined Sr, and Ti negative anomalies. These anomalies may be related to the fractionation of plagioclase (Sr), and/or Fe-Ti oxides (Ti). The distinctive depletion in Nb is a characteristic feature of arc granitoids. On the other hand, the REE patterns of the tonalite gneiss (Fig. 5d) are poorly-fractionated with (La/Yb)n ratio between 1.2 and 3.1 with no significant Eu anomalies (Eu/Eu* = 1 – 0.7). Their MORB patterns are nearly flat except for LILE enrichment and small negative Ti anomaly (Fig. 6d).

The syenites are characterized by high values of Al_2O_3 (17.7-18.3%), Na_2O (6.4-7.1%), K_2O (5.5-5.8%), Ba (904-2508 ppm), Hf (12-15 ppm), Zr (812-950 ppm), and total REE (142-782 ppm). Negative slopes of REE patterns characterize them (Fig. 5e) with LREE enrichment relative to HREE (Lan/Ybn ratios = 17.5 – 74), and positive Eu anomaly (Eu/Eu* = 1.0-2.03). The MORB normalized patterns (Fig. 6e) are strongly modified by fractionation as indicated by the negative anomalies of Sr and Ti. However, the high K, Ba and Eu contents may be attributed to K-feldspar accumulation in this rock variety.

Tectonic discriminantion diagram of Pearce and Cann (1973) shows that the metavolcanics and the metagabbro diorite rocks have remarkable similarities to calc-alkaline and island arc basalts (Fig. 7a). Discrimination between granitoids of various tectonic affinities has been proposed by Pearce *et al.,* (1984). On this diagram (Fig. 7b), the data points of the granite gneiss, tonalite gneiss and syenite plot within the field of Volcanic- Arc Granite (VAG); and thus have distinctive subduction-related signature.

3.2.2. Geochemistry of the granite ring dyke

On the Q-P diagram (Fig. 8a) of Debon and Le Fort (1983), the the rocks of the ring dyke are granites and adamellites. The alumina-saturation (Shand, 1927) of the ring dyke granites, measured by the molecular ratio Al_2O_3/ $CaO+Na_2O+K_2O$ (A/CNK), is plotted versus Al_2O_3/Na_2O+K_2O (Fig. 8b). Their A/CNK ratios show a wide range and fall in the peraluminous and peralkaline fields. Figure 9 shows the chemical data of some major and trace elements of the ring dyke granites plotted in Harker variation diagrams. Al_2O_3,

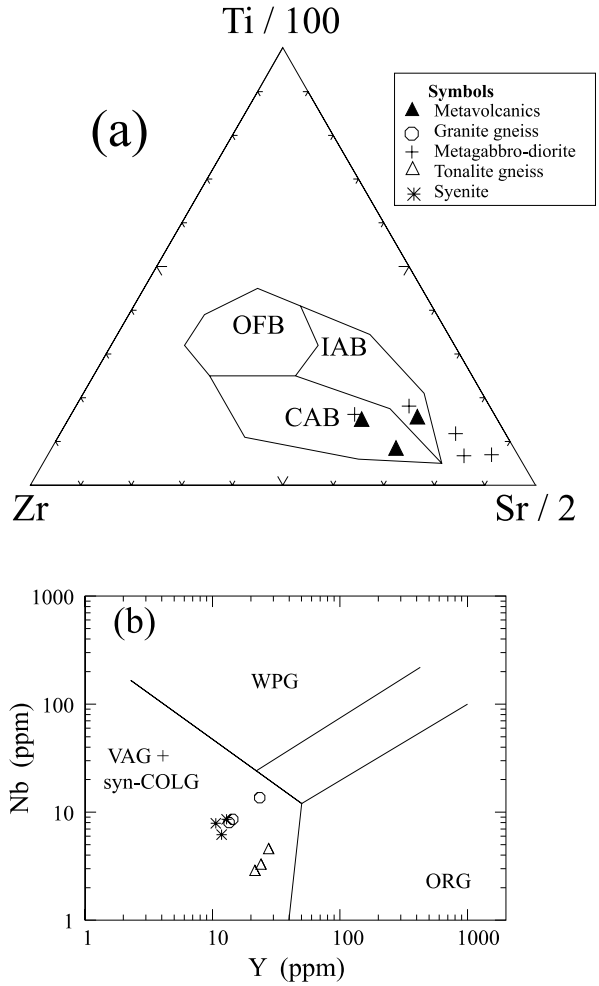

FIG. 7. Tectonic discrimination diagrams for the studied syn-tectonic igneous assemblage, (a) Zr-Ti-Sr diagram (Pearce and Cann, 1973), OFB = ocean floor basalts, IAB = island arc basalts, CAB = calc alkaline basalts. (b) Nb vs Y diagram (Pearce *et al.,* 1984), VAG = volcanic arc granite, sun-COLG = syn collision granite, ORG = ocean ridge granite, WPG = within plate granite. Symbols as in Fig. 3.

MgO, CaO, TiO_2, Sr and Ba show continuous decrease with increasing SiO_2 while K_2O and Rb increase with increasing SiO_2. Trends of Nb, and Zr are poorly developed in these granites, although a decrease in their contents with increasing SiO_2 can be noticed.

Chondrite-normalized REE patterns of the ring dyke granites are presented in Fig. 10a. In general, they are characterized by negative slopes of REE patterns with LREE enrichment relative to HREE (Lan/Ybn ratios = 28 – 7.3), poorly

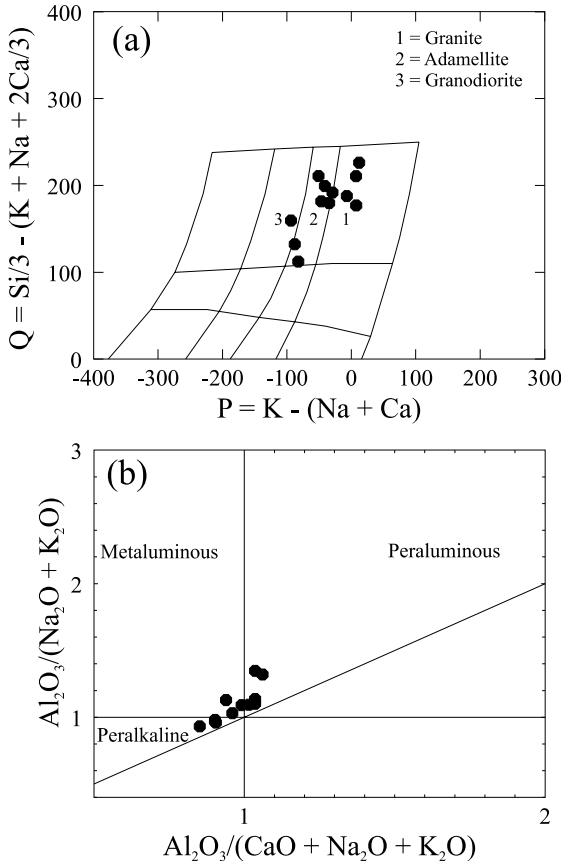

FIG. 8. (a) Q-P binary diagram (Debon and Le Fort, 1983) for the classification of the Turabah ring dyke granite, (b) A plot of Shand index for the studied granitoids; discrimination fields are from Maniar and Piccoli (1989).

fractionated HREE (Gdn/Ybn = 2-4) and moderate to large negative Eu anomaly (Eu/Eu* = 0.01-0.8). In the multi-element MORB-normalized diagrams (Fig. 10b), the ring dyke granites are characterized by high abundances of LILE (K, Rb and Ba) relative to HFSE (Zr, Ti and Y). Moreover, their patterns are highly modified by negative anomalies in Ba, Sr and Ti. The Ba and Sr depletion is consistent with early fractionation of plagioclase and K-feldspar, minerals, which readily accommodate both Ba and Sr (mineral/melt distribution coefficients are 6.1-12.9 and 3.6-3.9 respectively, Arth and Hanson, 1975; Mittlefehldt and Miller, 1983). The Ti anomaly, on the other hand, can be attributed to fractionation of Fe-Ti oxides.

The R1-R2 diagram (Fig. 11a) of de la Roche *et al.* (1980) with the calc-alkaline, subalkaline, and alkaline trends from Debon and Lemmet (1999)

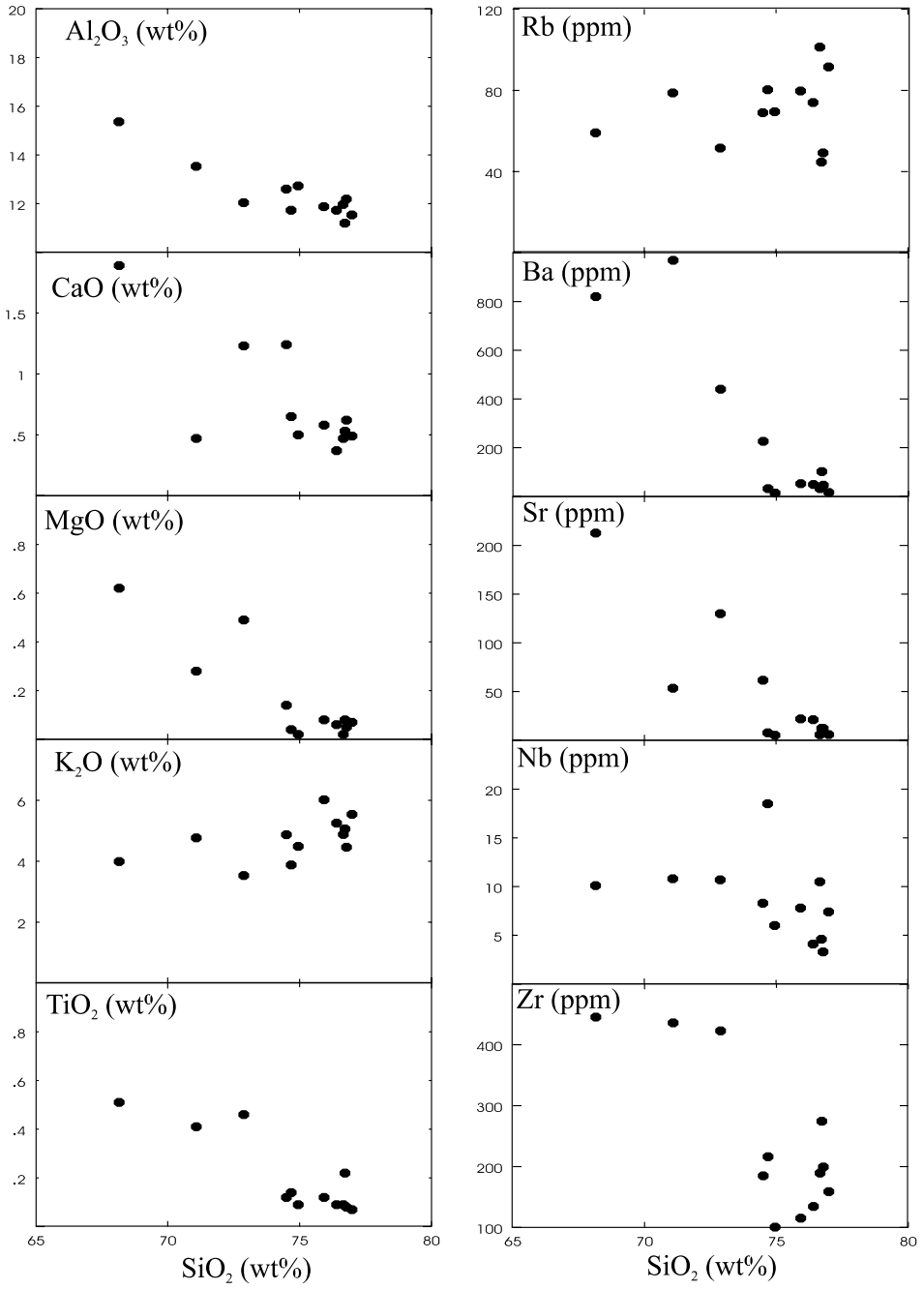

FIG. 9. Harker variation diagrams of some major and trace elements of the Turabah ring dyke granite.

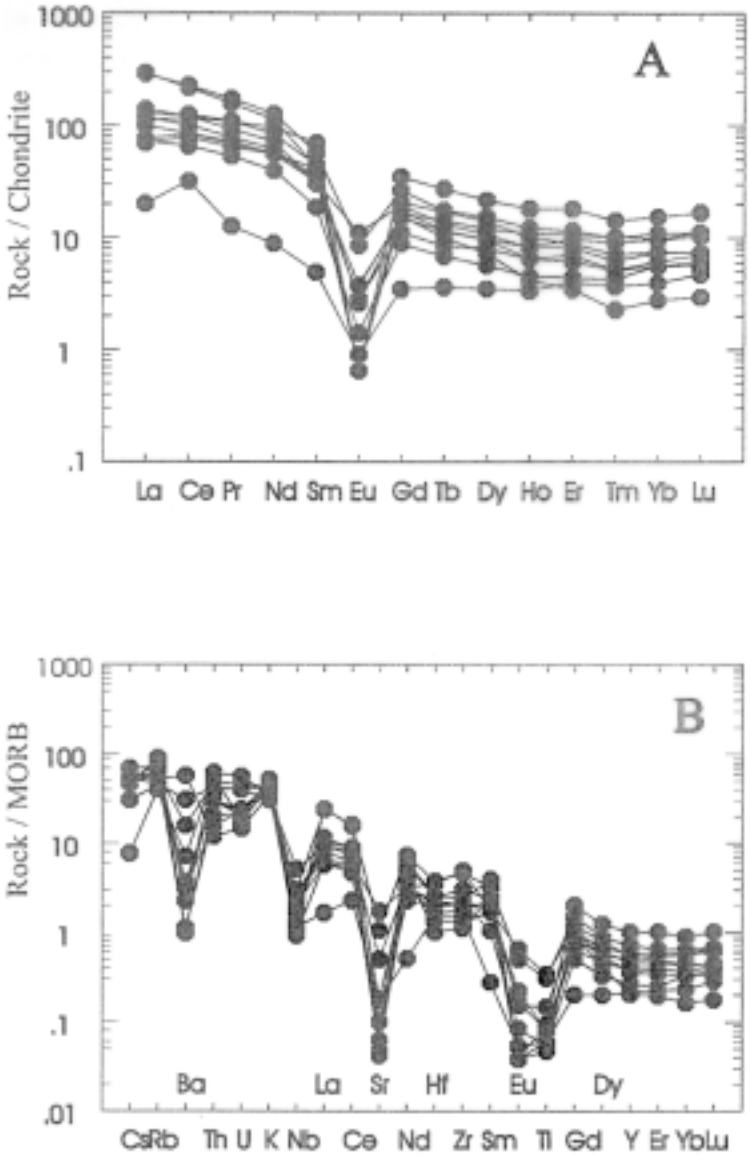

FIG. 10. (a) Chondrite-normalized REE patterns (Sun, 1982) and (b) N-MORB-normalized trace element plots (Sun and McDonough, 1989) for the Turabah ring dyke granite.

shows that the Turabah ring dyke granite samples are classified as alkali granites and lie within the anorogenic and post-orogenic granite fields. In the Zr + Nb + Ce + Y versus FeO*/MgO diagram (Fig. 11b) of Whalen *et al.* (1987), they are mainly classified as A-type granite.

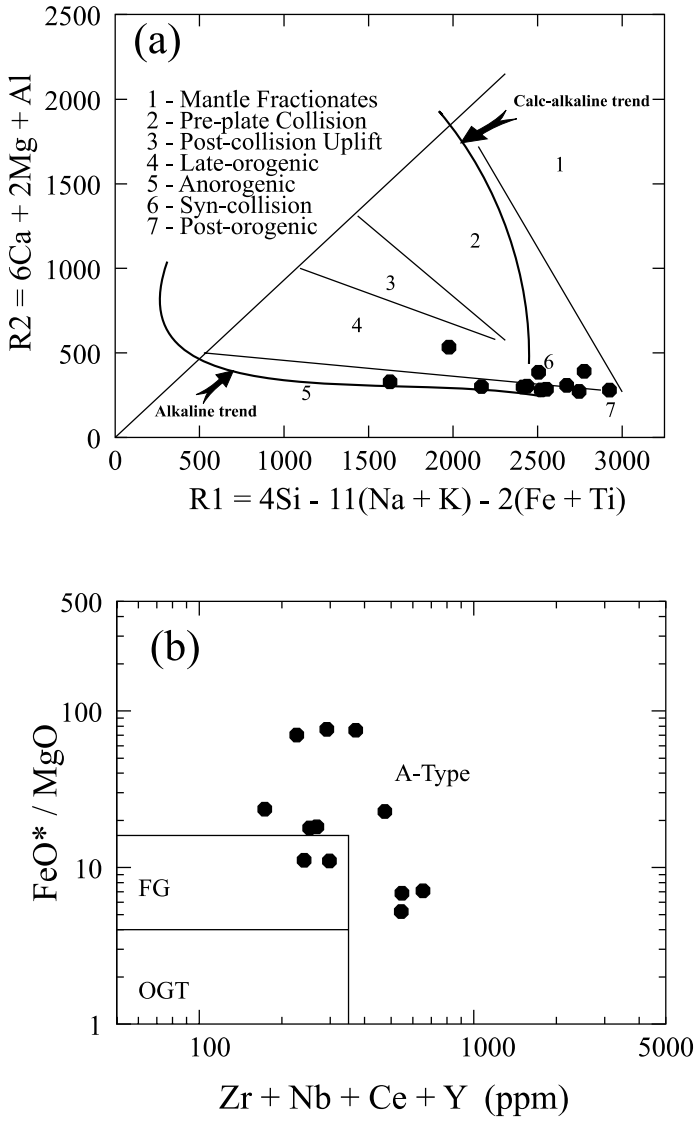

FIG. 11. (a) R1-R2 diagram (de la Roche *et al.,* 1980) with the alkaline, subalkaline and calc-alkaline trends from Debon and Lemmet (1999), (b) FeO*/MgO vs Zr + Nb + Ce + Y diagram (Whalen *et al.,* 1987).

4. Petrogenesis of The Syn-tectonic Igneous Assemblage

4.1. The Metavolcanics and the Metagabbro-diorite

The metavolcanics and the metagabbro-diorite show geochemical features characteristic of island arc setting. They are calc-alkaline and characterized by enrichment of the LILE (LREE, K, Rb, Ba and Sr) relative to the HFSE (HREE, Zr, Nb, and Y) and by K and Rb enrichment with increasing SiO_2. These features are consistent with modern calc-alkaline island arc suites. The parental magma of the these rocks is believed to have been generated by partial melting of the subducted slab or the mantle wedge above subduction zones that have been metasomatized by slab-derived fluids (Saunders *et al.,* 1980). The presence of wide chemical variations in the metavolcanics and cumulate features in the gabbro-diorite rocks are consistent with significant clinopyroxene (olivine), and plagioclase fractionation. Thus, crystal/melt fractional crystallization may explain the geochemical variations within the metavolcanics and metagabbro-diorite rocks.

4.2. The Granite and Tonalite Gneiss

The syn-tectonic granite gneiss shows the geochemical characteristics of calc-alkaline, subduction-related magmas and thus is regarded as pertaining to I-type products. Geochemical data show marked continuous trends in major and trace element abundances between the metagabbro-diorite and the granite gneiss (Fig. 12) suggesting that the two suites are genetically related through fractional crystallization processes. Because plagioclase feldspar and pyroxene are major fractionating phase in the evolution of the gabbroic rocks, there is an obvious decrease in the MgO and CaO contents from gabbro to granite gneiss (Fig. 12) suggesting that they evolved from the same magma by fractional crystallization. This is also supported by the REE patterns and the spidergrams (Figs. 5 and 6) of the two rock units, which show increase in Eu, Ti and Sr anomalies from the metagabbro-diorite to the granite gneiss.

On the other hand, geochemical data (Fig. 12) show marked discontinuities in major and trace element abundances between the tonalite gneiss and both of the gabbro-diorite and the granite gneiss, suggesting that they are genetically unrelated. If the metagabbro-diorite complex and the tonalite gneiss were related to each other by fractional crystallization processes, colinear trends should exist between SiO_2 vs K_2O, CaO and Zr, but such colinear relationships do not exist for the metagabbro-diorite and tonalite gneiss (Fig. 12). The tonalite gneiss samples are characterized by low contents of REE, Zr, Rb, Y, Nb and by a trace element patterns not modified greatly by fractionation, suggesting their derivation via partial melting of crustal material (Harris *et al.,* 1986). Crustal melting initiated by the intrusion of mantle-derived basaltic rocks is the most plausible physical model of crustal melting which can explain the generation of tonalite

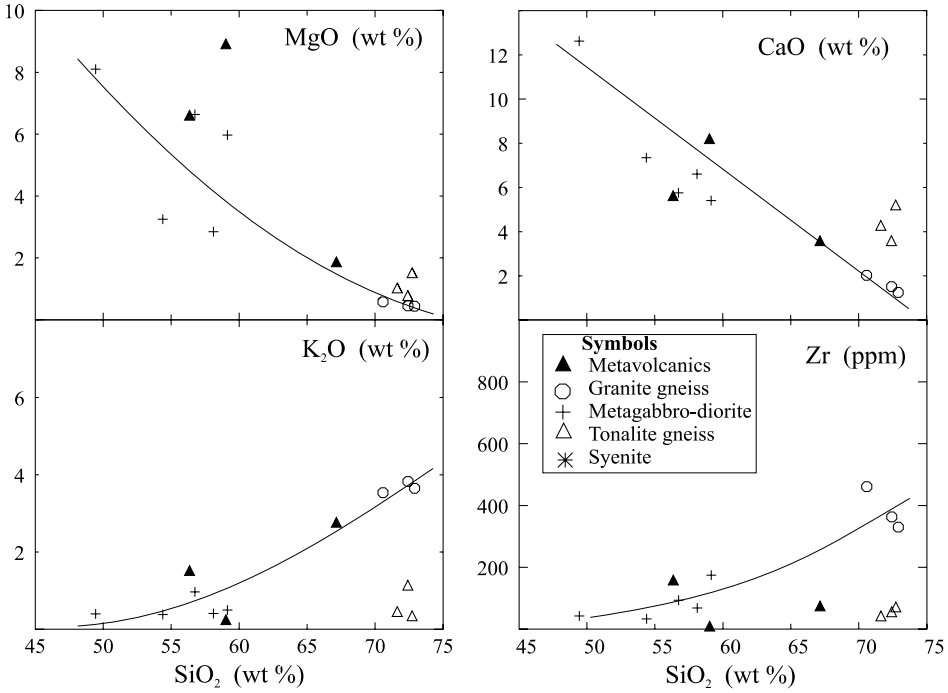

FIG. 12. Harker variations diagrams of some major and trace elements of the syn-tectonic igneous assemblage. Symbols as in Fig. 3.

gneiss melt in orogenic areas. In this model, underplating of basaltic magma at the Moho and the intrusion of mafic magma into the lower crust can serve as energy-transfer mechanism that initiate melting in the lower crust (Bergantz, 1989). This process is particularly applicable to tectonic environments, which contain large amount of mafic magmas such as volcanic arcs (Whitney, 1988). In this instance, it is worthy of mentioning that the emplacement of the tonalite gneiss body in the study area took place during the island arc stage. This means that this process is applicable for its origin.

5. Petrogenesis of the Ring Dyke A-type Granite

5.1. Evolution Processes

Many authors have discussed the mechanism of emplacement of the Turabah ring dyke. In explaining the origin of ring complexes and associated ring dyke, in volcanic terrains, the cauldron subsidence model (Turner and Bowden, 1979) is suggested. However, the present geochemical and field study as well as structural studies (Divi *et al.,* 1984) show that Turabah ring structure post-date the surrounding volcanic rocks and thus could not have developed due to cauldron

subsidence immediately after the eruption of the volcanic rocks. The most plausible model for the emplacement of the Turabah ring dyke is that proposed by Divi *et al.,* (1984) where polyphase deformation and metamorphism may be reflected in the form of Hertezizn fractures at depth followed by horizontal and vertical tension and lastly the development of quasi-oval fractures along which the ring dyke has been intruded.

In the normative Qz-Ab-Or system (Fig. 13), the Turabah ring dyke A-type granites plot along the polybaric granitic minima line at low pressure (Tuttle and Bowen, 1958). This distribution suggests that all the points are related by fractional crystallization. Other geochemical data cited above also suggest that the Turabah ring dyke A-type granites are extremely fractionated and their present composition is compatible with partitioning of elements between a silicic melt and minerals crystallizing from that melt (alkali feldspar, amphibole, titanomagnetite and apatite). This is true for the elements Ba, Sr, Eu, Nb, and Ti, which show strong negative anomalies on the spiderdiagram (Fig. 10b) or negative correlation with SiO_2 (Fig. 9). Other geochemical criteria that suggest the importance of fractional crystallization in the evolution of the Turabah ring dyke granite include: 1) the wide variations in the K/Sr, K/Ba, and Rb/Ba and their positive correlation with SiO_2 (Fig. 14) suggest the preponderate role of K-feldspar fractionation in the evolution of these granites, 2) the decrease of Eu/Eu* with increasing SiO_2 suggest the preponderate role of plagioclase feldspar fractionation, 3) incompatible (Zr) versus incompatible (Hf) trace element variations are linear (Fig. 14) with trends from low abundances in the least evolved samples towards higher abundances in highly evolved samples.

It is important to assess whether or not the examined A-type granites have undergone crustal contamination. This is because they have been intruded into thick continental crust and may have adequate opportunity to interact with crustal rocks during their emplacement through assimilation fractional crystallization processes. Available evidence suggests that contamination, through assimilation, has not affected the Turabah A-type granite pluton on a large scale. Few xenoliths in these granites have sharp contacts with the granitic rocks and contain abundant amphibole while there is very little amphibole in the granite. These xenoliths have mineralogical composition similar to the surrounding metavolcanic rocks. The linear correlation of Sr on the Harker diagram (Fig. 9) and its lower values (5-213 ppm) in the studied granites suggest that random assimilation with Sr-rich rocks such as those constituting the metavolcanic xenoliths was of minimal importance. Moreover, the low variation in the K/Rb ratio (Fig. 14) suggests that the trace element relations in these A-type granites are not affected much by crustal contamination.

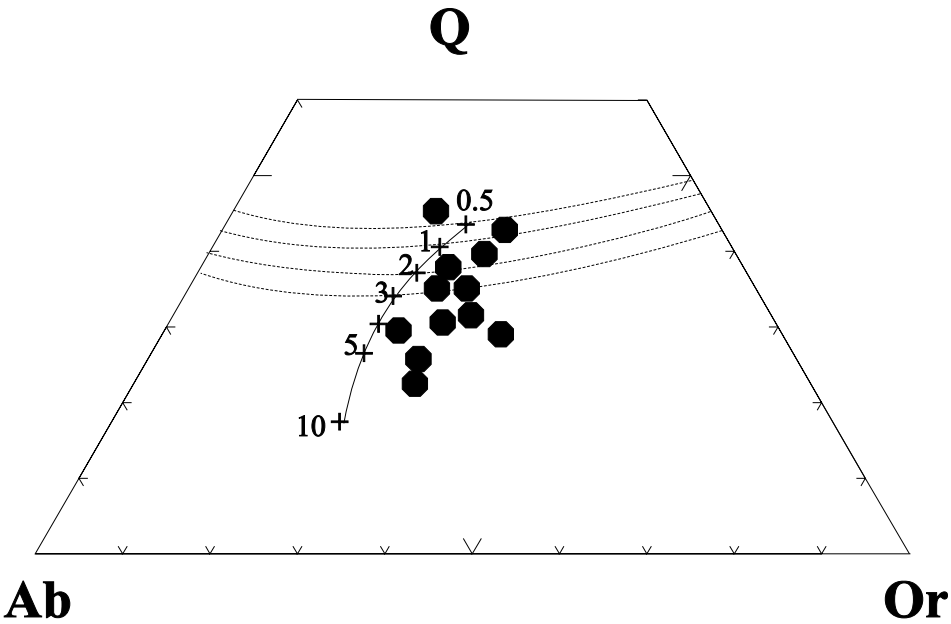

FIG. 13. Normative Q-Ab-Or composition of the Turabah ring dyke granite relative to experimental H_2O-saturated minimum melt composition (Anderson and Bender, 1989).

5.2. Source Rock

Many aspects of the Turabah A-type granites make the identification of their source materials very difficult. First, the granites are geochemically highly evolved and the magma has clearly undergone extensive differentiation since its formation. Second, the granites were emplaced at shallow crustal levels and their root zones are not exposed. This is in addition to the absence of mafic rocks of the same age as the granites. The aim of this section is thus to put broad constraints on possible sources of these granites, which can be inferred from the data presented in this paper and from previous studies.

It has been shown that the Turabah ring dyke A-type granites are evolved through fractional crystallization process from earlier I-type granitic to tonalitic magma without or with insignificant crustal contamination. Field and geochemical data show that the ring dyke granite differs from the surrounding earlier I-type granite and tonalite gneiss. Derivation of the A-type granite by extensive fractional crystallization from the less differentiated granite and tonalite gneiss can be thus ruled out by the difference in tectonic setting and different isotopic composition (i.e. initial $^{87}Sr/^{86}Sr$ ratios are 0.704 and 0.709 for the granite gneiss and ring dyke granite, respectively; (Radain *et al.,* 1988). Fractional crystallization of a mantle-derived mafic magma may produce granitic

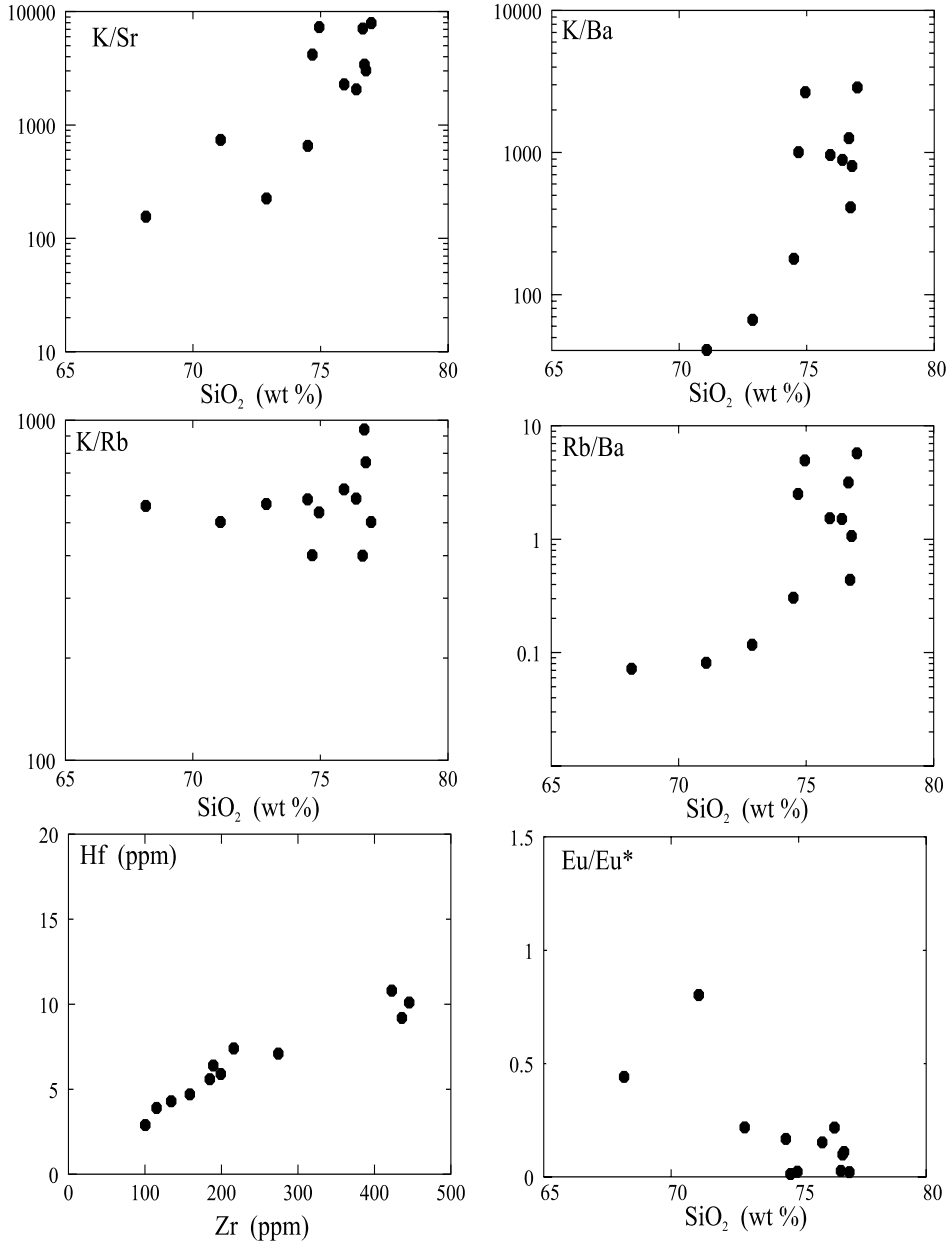

FIG. 14. SiO_2 vs K/Sr, K/Ba, K/Rb, Rb/Ba and Eu/Eu* and Zr vs Hf for the Turabah ring dyke granite.

melts with A-type characteristics (Turner *et al.,* 1992). However, the high initial $^{87}Sr/^{86}Sr$ ratio and the absence of mafic rocks of the same age as the ring dyke granite in the study area preclude this process.

Granitic rocks with A-type geochemical signatures have been interpreted as products of high temperature partial melting of a granulitic residue from which a granitoid melt was previously extracted (e.g. Collins *et al.,* 1982; Clemens *et al.,* 1986). However, the high contents of LILE (Table 1) in the investigated A-type granites preclude the derivation of these granites from a LILE-depleted granulitic residue in the lower continental crust, unless these elements have been enhanced by extreme fractionation of a depleted parental magma (Turner *et al.,* 1992). Sylvester, (1989) and Creaser *et al.* (1991) argued against the melt-depleted lower crust model and suggested that A-type granites may be better modelled by partial melting of an undepleted I-type tonalitic to granodioritic source. In Saudi Arabia, hornblende- and biotite-bearing I-type tonalites and granodiorites are common (Jackson, 1986) and can provide a suitable protolith for the A-type granites. However, the high initial $^{87}Sr/^{86}Sr$ ratio of the investigated granites rule out their derivation from tonalites and granodiorites with initial $^{87}Sr/^{86}Sr$ ratio of 0.702-0.704 (Duyverman *et al.,* 1982). The lower crust in the Arabian-Nubian Shield is juvenile (700-900 Ma) and composed of mafic layer of modified oceanic crust and mafic cumulates (Gettings *et al.,* 1986; McGuire and Stern, 1993). These rocks are attractive sources to produce melts of tonalitic melts with low SiO_2 content (52-55%) at lower crustal pressures (Wolf and Wyllie, 1994). Thus, a plausible explanation of the high initial $^{87}Sr/^{86}Sr$ ratio in the studied granites is their derivation by partial melting of mafic lower crust and direct contamination with an old continental crust beneath the Turabah region. This magma may be granodioritic or tonalitic that could have been derived by partial melting of lower crustal source or mantle-derived mafic magma.

In the Arabian-Nubian Shield there is no conclusive evidence for the presence of Archean or even Mid-Proterozoic crust in the central part of the Shield. Detailed isotopic studies (Stacey *et al.,* 1980; Stacey and Stoeser, 1983) proved the presence of old continental crust of at least early Proterozoic age in eastern and southern Saudi Arabia, Yemen, and Oman and to the west of Aswan in Egypt. This distribution has led Stacey and Stoeser (1983) to conclude that the Arabian-Nubian Shield has an oceanic core flanked by rocks that have developed from older continental crust. The Turabah ring-dyke granite, which occurs in the central part of the Arabian Shield, shows high initial $^{87}Sr/^{86}Sr$ of 0.7089 ± 0.0001. There is no explanation for this high initial ratio other than direct contamination with an old continental crust. This is because interaction with Pan-African rocks or even their partial melting cannot account for such

high initial ratio. Thus, it can be suggested that an old continental crust or micro continent may exist beneath the Turabah area. However, this needs further investigation using other isotope systems such as Sm/Nd and Pb/Pb in order to completely evaluate this speculation.

6. Conclusion

Petrological and geochemical studies of the Pan-African igneous complex in the Turabah area, central Arabian Shield of Saudi Arabia, reveal the presence of two rock groups, namely: (1) a syntectonic I-type magmatism represented by metavolcano-sedimentary association, metagabbro-diorite, granite gneiss, tonalite gneiss and syenite, and (2) an anorogenic A-type-granite represented by ring dyke.

The metavolcanic rocks and the metagabbro-diorite are calc-alkaline and were formed by fractional crystallization of a basaltic magma derived by partial melting of a metasomatized upper mantle in an island arc setting. The granite gneiss suite, on the other hand, was derived from the metagabbro-diorite rocks by fractional crystallization. The tonalite gneiss samples are characterized by low contents of REE, Zr, Rb, Y, Nb and by a trace element pattern not modified greatly by fractionation, suggesting their derivation via partial melting of crustal material (Harris *et al.,* 1986). Crustal melting initiated by the intrusion of mantle-derived basaltic is the most plausible physical model of crustal melting which can explain the generation of tonalite gneiss melt in orogenic areas. In this model, underplating of basaltic magma at the Moho and the intrusion of mafic magma into the lower crust can serve as energy-transfer mechanism that initiate melting in the lower crust

The Turabah ring dyke is a late Cretaceous anorogenic alkaline subsolvus monzo-and syenogranites. It was emplaced at shallow crustal levels in the syntectonic Pan-African igneous assemblage. The rocks of the ring dyke are geochemically evolved and enriched in Rb, Y, and Nb, thus leading to their classification as A-type granites. It is suggested that they could have been derived by fractional crystallization of granodioritic magma. Partial melting of a mafic lower crust followed by direct contamination with old continental crust in an extensional-related tectonic setting could form this granodioritic magma.

Acknowledgement

The author is greatly indebted to Prof. M. A. Hassanen for his valuable comments, constructive criticism and for reading the manuscript at various stages. Dr. A. Moghazi, Alexandria University, is deeply appreciated for reviewing the manuscript.

References

Aldrich, L.T. (1978) Radiometric age determinations of some rocks from the Arabian Shield. In: **Aldrich, L.T., Brown, G.F., Hedge, C.E.** and **Marvin, R.,** *Geochronologic data for the Arabian Shield,* Section 1: U.S. Geol. Surv., Saudi Arabian project Report 240, 9 p.

Anderson, J.L. and **Bender, E.E.** (1989) Nature and origin of Proterozoic A-type granitic magmatism in the south-western of the United States of America. *Lithos* **23:** 19-52.

Arth, J.G. and **Hanson, G.N.** (1975) Geochemistry and origin of the early Precambrian crust of northeastern Minnesotta. *Geochim. Cosmochim. Acta* **39:** 325-362.

Barker, F. (1979) Trondhjemite: definition, environment and hypothesis of origin. In: **Barker, F.** (Ed.), *Trondhjemites, dacites and related rocks*. Elsevier, Amsterdam. 1-12

Bergantz, G.W. (1989) Underplating and partial melting: implications for melt generation and extraction. *Science* **245:** 1093-1095

Bokhari, F.Y. and **Kramers, J.D.** (198) Island arc character and later Precambrian age of volcanics of wadi Shuwas, Hijaz, Saudi Arabia ñ Geochemical and Sr and Nd isotope evidence. *Earth Planet. Sci. Lett.* **54:** 409-422.

Cater, F.W. and **Johnson, P.R.** (1987) *Geologic map of the Jabal Ibrahim quadrangle, sheet 20 E,* Kingdom of Saudi Arabia. Saudi Arabian Dir. Gen. Miner. Resour. Map GM-96C.

Clemens, J.D., Holloway, J.R. and **White, A.J.R**. (1986) Origin of an A-type granite: experimental constraints. *Am. Miner.* **79:** 71-86

Collins, W.J., Beams, S.D., White, A.J.R. and **Chappell, B.W.** (1982) Nature and origin of A-type granites with particular reference to southeastern Australia. *Contrib Mineral Petrol* **80:** 189-200

Creaser, R.A., Price, R.C. and **Wormald, R.J.** (1991) A-type granite revisited: assessment of residual source model. *Geology* **19:** 163-166

de la Roche, H., Leterrier, J., Grandelaude, P. and **Marchal, M.** (1980) A classification of volcanic and plutonic rocks using R1-R2 diagram and major-element analyses – its relationships with current nomenclature. *Chem. Geol.,* **29:** 183 - 210.

Debon, F. and **Lemmet, M.** (1999) Evolution of Mg/Fe ratios in late Variscan plutonic rocks from external crystalline massifs of the Alps (France, Italy, Switzerland). *J. Petrol.* **40:** 1151-1185.

Debon, F. and **Le Fort, P.** (1983) A chemical-mineralogical classification of common plutonic rocks and their magmatic associations. *Transaction of the Royal Society of Edinburgh, Earth Science* **73:** 135-149.

Divi, S.R., Alwashe, M., Basahel, A.N. and **Groen, C.** (1984) Deformational structures within and outside a ring structure, Wadi Turabah, Central Arabian Shield. *Bull. Instit. Appl. Geol. King Abdulaziz Univ. Jeddah* **6:** 397-4073.

Duyverman, H.J., Harris, N.B.W. and **Hawkesworth, C.J.** (1982) Nd and Sr isotope evidence from the Arabian Shield. *Earth Planet. Sci. Lett.* **59:** 315-326.

Fleck, R.J., Coleman, R.G., Cornwall, H.R., Greenwood, W.R. and **Hadley, D.G.** (1976) Geochronology of the Arabian shield, western Saudi Arabia: K/Ar results. *Geol. Soc. Am. Bull.* **87:** 9-21.

Fleck, R.J., Greenwood, W.R., Hadley, D.G., Andersen, R.E. and **Schmidt, D.L.** (1980) Age and evolution of the southern part of the Arabian Shield. *Instit. Appl. Geol. Jeddah Bull.* **3:** 1-17.

Frisch, W. and **Al Shanti, A.** (1977) Ophiolite belts and the collision of island arcs in the Arabian Shield. *Tectonophysics* **43:** 293-306.

Gettings, M.E., Blank, H.R., Mooney, W.D. and **Healey, J.H.** (1986) Crustal structure of southwestern Saudi Arabia. *Jour. Geoph. Res.* **91:** 6491 - 6512.

Greene, R.C. and **Gonzalez, L.** (1980) *Reconnaissance geology of the wadi Shuqub quadrangle,* sheet 21/41 A. Kingdom of Saudi Arabia. Saudi Arabian Dir. Gen. Miner. Resour., Map GM-54.

Harris, N.M. (1985) Alkaline complexes from the Arabian Shield. *J Afr Earth Sci.* **3:** 83-88.

Irvine, T.N. and **Baragar, W.R.** (1971) A guide to the chemical classification of the common volcanic rocks. *Can. J. Earth Sci.* **8:** 523-548.

Jackson, N.J. (1986) Petrogenesis and evolution of Arabian felsic plutonic rocks. *J African Earth Sci.* **4:** 47-59

Kröner, A., Greiling R., Reischmann T., Hussein, I. H., Stern, R. J., Durr, S., Kruger, J. and **Zimmer, M.** (1987) Pan-African crustal evolution in the Nubia segment of northeast Africa. In: **Kröner, A.** (ed). Proterozoic lithospheric evolution, *Am Geophys Union Geodynamics Series* **17:** 235-257.

Kröner, A. (1985) Ophiolites and the evolution of tectonic boundaries in the late proterozoic Arabian-Nubian Shield of northeast Africa and Arabia. *Precamb. Res.* **27:** 277-300.

Kroner, A., Halpern, M. and **Basahel, A.** (1984) Age and significance of metavolcanic sequences and granitoid gneisses from the Al-Lith area, Southwestern Arabian Shield. *King Abdulaziz Univ,, IGCP Project* **164:** 380-388.

Le Bas, M.J., Le Maitre, R.W., Streckeisen, A. and **Zanethin, B.** (1986). A chemical classification of volcanic rocks based on total alkali-silica diagram. *J. Petrol.* **27:** 745-750.

Maniar, P.D. and **Piccoli, P.M.** (1989) Tectonic discrimination of granitoids. *Geol. Soc. Am. Bull.* **101:** 635-643

Marzuki, F.H.M., Jackson, N.J., Ramsay, C.R. and **Darbyshire, D.P.F.** (1982) Composition, age and origin of two Proterozoic diorite-tonalite complexes in the Arabian Shield. *Precamb. Res.* **19:** 31-50.

McGuire, A.V. and **Stern, R.J.** (1993) Granulite xenoliths from western Saudi Arabia: the lower crust of the late Precambrian Arabian-Nubian Shield. *Contrib. Mineral. Petrol.* **114:** 395- 408.

Mittlefehldt, D.W. and **Miller, C.F.** (1983) Geochemistry of the sweetwater wash pluton, California: implication for anomalous trace element behaviour during differentiation of felsic magmas. *Geochim. Cosmochim. Acta* **47:** 109 - 124.

O'Conner, J.T. (1965) A classification for quartz-rich igneous rocks based on feldspar ratios. *US Geol. Surv., Prof. Pap.,* **525-B:** 79-84.

Pearce, J.A., Harris N.B.W. and **Tindle, A.G.** (1984) Trace element discrimination diagrams for the tectonic interpretation of granitic rocks. *J. Petrol* **25:** 956-983

Pearce, J.A. (1983) The role of subcontinental lithosphere in magma genesis at destructive plate margins. In: **Hawkesworth C. J.** and **Norry, H. J.** (eds): *Continental basalt and mantle xenoliths,* 230-249, Nantwich, Shiva.

Pearce, J.A. and **Cann, J.R.** (1973) Tectonic setting of basic volcanic rocks determined using trace element analyses. *Earth Planet. Sci. Lett.* **19:** 290-300.

Radain, A.A., Ali, S. and **Abdel Monem, A.A.** (1988) Geochronology and Geochemical evolution of the Wadi Turabah felsic plutonic ring complex, Central Arabian Shield. *J.KAU: Earth Sci.,* **1:** 1-25.

Radain, A.A. and **Nasseef, A.O.** (1982) Geochronology and geochemistry of wadi Shuqub granitic rocks, west-central Arabian Shield. *Precamb. Res.* **16:** A 35 (Abstract)

Radain, A.A., Ali, S., Nasseef, A.O. and **Abdel-Monem, A.A.** (1987) Rb-Sr geochronology and geochemistry of plutonic rocks from wadi Shuqup quadrangle, west-central Arabian Shield. *J. Afr. Earth Sci.* **6:** 553-568.

Ramsay, C.R., Basahel, A.N. and **Jackson, N.J.** (1981) Petrography, geochemistry and origin of volcano-sedimentary succession between Jabal Ibrahim and Al-Aqiq, Saudi Arabia. *Bull. Instit. Appl. Geol. King Abdulaziz Univ. Jeddah* **4:** 1-24.

Saunders, A.D., Tarney, J. and **Weaver, D.** (1980) Transverse geochemical variations across the Antractic Peninsula: implications for the genesis of calcalkaline magmas. *Earth Planet. Sci. Lett.* **46:** 344-360.

Shand, S.J. (1927) *The eruptive rocks,* 1st edition. New York: John Wiley, 488 p.

Stacey, J.S., Doe, B.R., Roberts, R.J., Delevaux, M.H. and **Gramllch, J.W.** (1980) A lead isotope study of mineralization in the Saudi Arabian Shield. *Contrib.. Mineral. Petrol.* **74:** 175-188.

Stacey, S.J. and **Stoeser, B.S.** (1983) Distribution of oceanic and continental leads in the Arabian-Nubian Shield. *Contrib. Mineral. Petrol.* **84:** 91-105.

Stern, R.J. (1994) Arc assembly and continental collision in the Neoproterozoic East African Orogen: Implications for the consolidation of Gondwanaland. *Ann Rev Earth Planet Sci.* **22:** 319-351

Stoeser, D.B. and **Camp, V.E.** (1985) Pan-African microplate accretion of the Arabian Shield. *Geol. Soc. Am. Bull.* **96:** 817-826.

Stoeser, D.B. and **Elliott. J.E.** (1980) Post-orogenic peralkaline and calc-alkaline granites and associated mineralizations of the Arabian Shield, Kingdom of Saudi Arabia. *Bull. Instit. Appl. Geol. King Abdulaziz Univ. Jeddah* **4:** 1-23.

Sun, S.S. (1982) Chemical composition and origin of the Earth's primitive mantle. *Geochim. Cosmochim. Acta* **46**: 179-192.

Sun, S.S. and **McDonough, W.E.** (1989) Chemical and isotopic systematics of oceanic basalts: implications for mantle composition and processes. In: **Saunders, AD** and **Norry, MJ** (eds.) *Magmatism in the oceanic basins. Geol Soc Spec Publ* **42:** 313-345.

Sylvester, P.J. (1989) Post-collisional alkaline granites. *J. Geol.* **97:** 261-280

Turner, S.P., Foden, J.D. and **Morrison, R.S.** (1992) Derivation of some A-type granites by fractionation of basaltic magma: an example from the Padthaway Ridge, South Australia. *Lithos* **28:** 151-179

Turner, D.C. and **Bowden, P.** (1979) The Ningi-Burra complex, Nigeria, dissected calderas and migrating magmatic centers. *J. Geol. Soc. London* **136:** 105-119.

Tuttle, D.F. and **Bowen, N.L.** (1958) Origin of granites on the light of experimental studies in the system $NaAlSi_3O_8$-$KAlSi_3O_8$-SiO_2-H_2O. *Geol. Soc. Am. Mem.* **74:** 130- 142.

Vail, J.R. (1985) Pan-African (Late Precambrian) tectonic terrains and the reconstruction of the Arabian-Nubian shield. *Geology* **13:** 839-842.

Whalen J.B., Currie, K.L. and **Chappell, B.W. (**1987) A-type granites: geochemical characteristics, discrimination and petrogenesis. *Contrib Mineral Petrol* **95:** 407-419

Whitney, J.A. (1988) The origin of granite: the role and source of water in the evolution of granitic magmas. *Geol. Soc. Am. Bull.* **100:** 1886-1897.

Wolf, M.B. and **Wyllie, P.J.** (1994) Dehydration-melting of amphibolites at 10 kbar: the effects of temperature and time. *Contrib Mineral Petrol* **115:** 369-383

قاطع تربه الحلقي من العصر الكريتاوي المتأخر في وسط الدرع العربي - جيولوجيته وجيوكيميائيته والدلالات التكتونية له.

عصام يحيى الفيلالي

كلية علوم الأرض ، جامعة الملك عبدالعزيز ، جـــدة - المملكة العربية السعودية

المستخلص. إن قاطع تربة الحلقي في وسط الدرع العربي بالمملكة العربية السعودية هو جرانيت من نوع (A) من العصر الكريتاوي المتأخر، ولقد اخترق هذا القاطع على مستويات قشريه ضحله مجموعة من الصخور البركانية - الرسوبية الكلسقلوية المهشمه نتيجة تجمع تكتوني متزامن مع الحمى الإفريقي وكذا صخور الميتاجابرو - ديوريت والجرانوديوريت والجرانيت والتونالیت النيسي والسيانيت . لقد أظهرت صخور البركانيات المتحوله والميتاجابرو - ديوريت خصائص بترولوجيه وجيوكيميائية تشير إلى أنها نشأت من صخور قوس جزرية ذات مصدر وشاحي تكونت بعملية انصهار جزئي لهذا الوشاح فوق نطاق انضواء أما صخور الجرانوديوريت - الجرانيت النيسيى فهو جرانيت كلسقلوى من نوع (I) وهذه الصخور مع صخور الميتاجابرو - الديوريت تبين اتجاه متصل في انتشار وتوزيع العناصر الأساسية وكذا العناصر الشحيحه مما يشير إلى أن هذه الصخور ذات أصل مشترك يرجع إلى عملية التبلور التجزيئي. أما صخور التونالیت النيسي فتبين محتوى منخفض في العناصر الأرضية النادرة (٥١-٧٤ جزء في المليون) والزيركونيوم (٤٣-٧٢ جزء في المليون) وأكسيد البوتاسيوم (٠,٣٥ - ١,١٤ في المائة) والنيوبيوم (٣-٥ جزء في المليون) كما أنها تبين هيئة توزيع للعناصر الشحيحة مشابهة لتلك التي لم تتأثر كثيراً بعملية التبلور التجزيئي . هذه المظاهر الجيوكيميائية تشير إلى أن هذه الصخور قد نشأت من عملية انصهار جزئي لمواد قشرية .

إن صخور قاطع تربة الحلقي تتكون من مونزو إلى سيانوجرانيت متطورة من الناحية الجيوكيميائية (ثاني أكسيد السيلكون ٦٨ - ٧٧٪) وذات صفات ميتاألومينية إلى شبه فوق قلوية وتبين خصائص مشابهة

للجرانيت – A المتكون بين الألواح مع إثراء في أكسيد الحديديك (١ – ٤٪) ، الإيتريوم (٧– ٣٥ جزء في المليون) والنيوبيوم (٣– ١٩ جزء في المليون) والروبيديوم (٤٥– ١٠١ جزء في المليون) والزيركونيوم (١٠١– ٤٤٦ جزء في المليون) وكذا افتقار في أكسيد الكالسيوم (٠,٥ – ٩,١٪) وأكسيد المغنسيوم (٠,٢ –٠,٦٪) والباريوم (١٤– ٨٢٠ جزء في المليون) والاسترنشيوم (٥ – ٢١٣ جزء في المليون) .

إن النموذج الذي يتضمن انصهاراً جزئياً للقشرة القارية السفلية القاعدية في بيئة شد لتعطي صهير الجرانوديوريت يمكن أن تشرح أصل هذه الصخور. إن التلوث بقشرة قارية قديمة متبوعة بالتبلور التجزيئي قد لعب دوراً مهماً في تطور وإظهار المميزات الكيميائية في جرانيتات تربه. كما أن التطور المعقد في تاريخ المنطقة يمكن أن ينعكس في تكوين الكسور والتشققات الشبه بيضاوية والتي اخترقها الصهير المتمايز معطياً التركيب الحلقي في المنطقة.